11 Quantum Compass and Kitaev Models

Jeroen van den Brink and Zohar Nussinov
Institute for Theoretical Solid State Physics
IFW Dresden
Department of Physics, Washington University
St. Louis, Missouri 63160, USA

Contents

E. Pavarini and E. Koch (eds.)
Orbital Physics in Correlated Matter
Modeling and Simulation Vol. 13
Forschungszentrum Jülich, 2023, ISBN 978-3-95806-689-2
http://www.cond-mat.de/events/correl23

1 Introduction to compass models

Compass models are theories of matter in which the couplings between the internal spin (or other relevant field) components are inherently spatially (typically, direction) dependent. A simple illustrative example is furnished by the *90° compass model* on a square lattice in which only couplings of the form $\tau_i^x \tau_j^x$ (where $\{\tau_i^a\}_a$ denote Pauli operators at site i) are associated with nearest neighbor sites i and j separated along the x axis of the lattice while $\tau_i^y \tau_j^y$ couplings appear for sites separated by a lattice constant along the y axis. A very well-known compass model is the honeycomb Kitaev Hamiltonian. Such compass-type interactions can appear in diverse physical systems. This includes Mott insulators with orbital degrees of freedom where interactions sensitively depend on the spatial orientation of the orbitals involved, the low energy effective theories of frustrated quantum magnets, vacancy centers and cold atomic gases. Kitaev models, in particular the compass variant on the honeycomb lattice, realize basic notions of topological quantum computing. The fundamental inter-dependence between internal (spin, orbital, or other) and external (i.e. spatial) degrees of freedom which underlies compass models generally leads to very rich behaviors including the frustration of (semi-)classical ordered states on non-frustrated lattices and to enhanced quantum effects prompting, in certain cases, the appearance of zero temperature quantum spin liquids. As a consequence of these frustrations, new types of symmetries and their associated degeneracies may appear. In particular, these systems feature *intermediate* (more recently also referred to (especially in the high-energy and quantum information communities) and further classified as "higher form" or "subsystem") symmetries that lie midway between the extremes of global symmetries and local gauge symmetries and lead to effective dimensional reductions. We consider compass models in a unified manner, paying close attention to consequences of these symmetries, and to thermal and quantum fluctuations that stabilize orders via *order out of disorder* effects. We review non-trivial statistics and the appearance of *topological quantum orders* in compass systems in which, by virtue of their intermediate symmetry, standard orders do not arise.

Different physical contexts motivate compass models and they can emerge as low-energy effective models of systems with strongly interacting electrons. There are quite a few classes of materials where the microscopic interactions between electrons are described by an extended Hubbard model. Typically such materials contain transition-metal ions. Hubbard-type models incorporate both the hopping of electrons from lattice-site to lattice-site and the Coulomb interaction U between electrons that meet on the same site, typically the transition-metal ion. Particularly in the situation that electron-electron interactions are strong, effective low-energy models can be derived by expanding the Hubbard Hamiltonian in $1/U$, the inverse interaction strength. In such a low-energy model the interactions are only between the remaining *spin* and *orbital* degrees of freedom of the electrons. Compass model Hamiltonians arise when orbital degrees of freedom interact with each other.

In the situation that both orbital and spin degrees of freedom are present and their interactions are intertwined, the Kugel-Khomskii models arise [1]. Such models are relevant for strongly correlated electron systems such as transition metal (TM) oxides, when the low-energy electronic

behavior is dominated by the presence of very strong electron-electron interactions. The orbital degrees of freedom can be represented via pseudo-spins.
So-called e_g and t_{2g} orbital degrees of freedom that can emerge in transition metal compounds with electrons in partially filled TM d-shells, give rise to two-flavor compass models (for e_g) and to three-flavor compass models (for t_{2g}) [2–5]. Precisely these type of compass models also emerge in the study of systems of cold atoms in optical traps.

1.1 Definition of compass models

In order to define quantum compass models, we start by considering a lattice with sites on which quantum degrees of freedom live. Throughout this chapter the total number of lattice sites is denoted by N. Each lattice site has a vector pointing to it that is denoted by $\boldsymbol{r}$. When square (or cubic) lattices will be involved, these will be considered of dimension $N = L\times L$ (or $N = L\times L\times L$). On more general lattices, L denotes the typical linear dimension (i.e., linear extent along one of the crystal axis). We set the lattice constant to unity. The spatial dimensionality of the lattice is denoted by D (e.g., $D = 2$ for the square and honeycomb lattices, $D = 3$ in cubic and pyrochlore lattices etc.).
Depending on the problem at hand, we will refer to these degrees of freedom at the lattice sites as spins, pseudospins or orbitals. We denote these degrees of freedom by $\boldsymbol{\tau}_i$, where i labels the lattice sites and $\boldsymbol{\tau} \equiv \frac{1}{2}(\sigma^x, \sigma^y, \sigma^z)$, where σ^x, σ^y and σ^z are the Pauli matrices. In terms of the creation ($c^\dagger_\alpha$) and annihilation (c_α) operator for an electron in state α, the pseudospin operator $\boldsymbol{\tau}$ can be expressed as $\boldsymbol{\tau} = \frac{1}{2}\sum_{\alpha\beta} c^\dagger_\alpha \boldsymbol{\sigma}_{\alpha\beta} c_\beta$, where the sum is over the two different possibilities for each α and β. Here $\boldsymbol{\tau}$ is the fundamental $T = 1/2$ representation of SU(2), for $T > 1/2$ we use $\boldsymbol{T}$. A representation in terms of Pauli matrices is particularly useful for degrees of freedom that have two flavors, for instance two possible orientations of a spin (up or down) or two possible orbitals that an electron can occupy, as the Pauli matrices are generators of SU(2), the group of 2×2 matrices with determinant one. In most works in the field, it is common to explicitly label components of $T = 1/2$ degrees of freedom at different sites by $\sigma^\gamma_{\mathbf{r}}$. Following suite, we will at times (especially when discussing excitations in Kitaev's honeycomb model and its non-Abelian phase), interchangeably also use this more conventional notation. For degrees of freedom with n flavors, it makes sense to use a representation in terms of the generators of SU(n), which for the particular case of $n = 3$ are the eight Gell-Mann matrices λ_i, with $i = 1, 8$.
The name that one chooses to bestow upon the degree of freedom (whether *spin*, *pseudospin*, *color*, *flavor* or *orbital*) is of course mathematically irrelevant. For SU(2) quantum compass models it is important that the components of $\boldsymbol{\tau}$ obey the well-known commutation relation $[\tau^x, \tau^y]=i\tau^z$ and its cyclic permutations, and that $(\tau^\gamma)^2 = 1/4$ for any component $\gamma=x$, y or z. In the case of SU(3), in the fundamental representation $\boldsymbol{T}$ is the eight component vector $\boldsymbol{T}=\frac{1}{2}\sum_{\alpha\beta} c^\dagger_\alpha \boldsymbol{\lambda}_{\alpha\beta} c_\beta$, with commutation relations governed by those of the Gell-Mann matrices.
Compass models are characterized by the specific form that the interaction between the degrees of freedom assumes: (i) there is only an interaction between certain *vector components* of $\boldsymbol{\tau}$ and (ii) on different bonds in the lattice, different vector components interact. When, for instance,

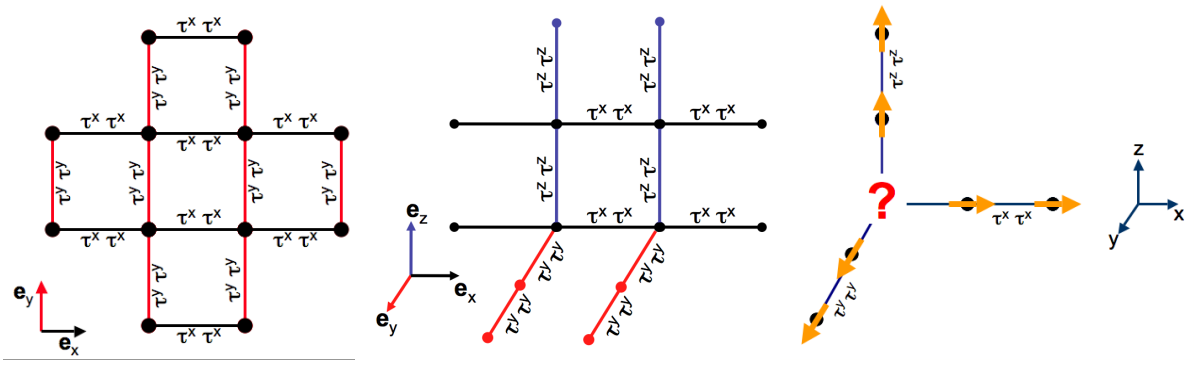

Fig. 1: *Left: The planar 90° compass model on a square lattice: the interaction of (pseudo-)spin degrees of freedom* $\boldsymbol{\tau} = (\tau^x, \tau^y)$ *along horizontal bonds that are connected by the unit vector* $\boldsymbol{e}_x$ *is* $\tau^x_{\boldsymbol{r}}\tau^x_{\boldsymbol{r}+\boldsymbol{e}_x}$. *Along vertical bonds* $\boldsymbol{e}_y$ *it is* $\tau^y_{\boldsymbol{r}}\tau^y_{\boldsymbol{r}+\boldsymbol{e}_y}$. *Middle: The 90° compass model on a cubic lattice: the interaction of (pseudo-)spin degrees of freedom* $\boldsymbol{\tau} = (\tau^x, \tau^y, \tau^z)$ *along horizontal bonds that are connected by the unit vector* $\boldsymbol{e}_x$ *is* $J\tau^x_i\tau^x_{i+\boldsymbol{e}_x}$. *On bonds connected by* $\boldsymbol{e}_y$ *it is* $J\tau^y_i\tau^y_{i+\boldsymbol{e}_y}$ *and along the vertical bonds it is* $J\tau^z_i\tau^z_{i+\boldsymbol{e}_z}$. *Right: Frustration in the 90° compass model on a cubic lattice. The interactions between pseudospins* $\boldsymbol{\tau}$ *are such that they tend to align their components* τ^x, τ^y *and* τ^z *along the* x, y *and* z*-axis, respectively. This causes mutually exclusive ordering patterns.*

a site i is linked to nearest neighbor sites j and k, the interaction along the lattice link $\langle ij\rangle$ can be of the type $\tau^x_i\tau^x_j$, whereas on the link $\langle ik\rangle$ it is $\tau^y_i\tau^y_k$. In the following sections specific Hamiltonians corresponding to various quantum compass models are introduced, in particular the 90° compass models, Kitaev's honeycomb model, 120° compass models and a number of generalizations thereof.

1.2 90° compass models

A basic realization of a quantum compass model can be set up on a two-dimensional square lattice, where every site has two horizontal and two vertical bonds. If one defines the interaction along horizontal lattice links $\langle ij\rangle_H$ to be $J\,\tau^x_i\tau^x_j$ and along the vertical links $\langle ij\rangle_V$ to be $J\,\tau^y_i\tau^y_j$, we have constructed the so-called *two-dimensional 90° quantum compass model* also known as the *planar 90° orbital compass model*, see Fig. 1. Its Hamiltonian is

$$H^{90^\circ}_{\square} = -J_x \sum_{\langle ij\rangle_H} \tau^x_i\tau^x_j - J_y \sum_{\langle ij\rangle_V} \tau^y_i\tau^y_j. \tag{1}$$

The isotropic variant of this system has equal couplings along the vertical and horizontal directions ($J_x = J_y = J$). The minus signs that appear in this Hamiltonian were chosen such that the interactions between the pseudospins $\boldsymbol{\tau}$ tend to stabilize uniform ground states with "ferro" pseudospin order. (In $D = 2$ the 90° compass models with "ferro" and "antiferro" interactions are directly related by symmetry). For clarity, we note that the isotropic two-dimensional compass model is very different from the two-dimensional Ising model

$$H^{Ising}_{\square} = -J \sum_{\langle ij\rangle_H} \tau^x_i\tau^x_j - J \sum_{\langle ij\rangle_V} \tau^x_i\tau^x_j = -J \sum_{\langle ij\rangle} \tau^x_i\tau^x_j,$$

where on each horizontal and vertical vertex of the square lattice the interaction is the same and of the form $\tau_i^x \tau_j^x$. It is also very different from the two-dimensional XY model

$$H_{\square}^{XY} = -J \sum_{\langle ij\rangle_H, \langle ij\rangle_V} (\tau_i^x \tau_j^x + \tau_i^y \tau_j^y),$$

because also in this case the interaction terms in the Hamiltonian are the same on all bonds.
One can rewrite the 90° compass Hamiltonian in a more compact form by introducing the unit vectors $\boldsymbol{e}_x$ and $\boldsymbol{e}_y$ that denote the bonds along the x- and y-direction in the 2D lattice, so that

$$H_{\square}^{90^\circ} = -J \sum_{\boldsymbol{r}} (\tau_{\boldsymbol{r}}^x \tau_{\boldsymbol{r}+\boldsymbol{e}_x}^x + \tau_{\boldsymbol{r}}^y \tau_{\boldsymbol{r}+\boldsymbol{e}_y}^y), \tag{2}$$

where the sum over $\boldsymbol{r}$ represents the sum over lattice sites and every is bond counted only once. With this notation the compass model Hamiltonian can be cast in the more general form

$$H_{\square}^{90^\circ} = -J \sum_{\boldsymbol{r},\gamma} \tau_{\boldsymbol{r}}^\gamma \tau_{\boldsymbol{r}+\boldsymbol{e}_\gamma}^\gamma, \tag{3}$$

where for the 90° square lattice compass model, $H_{\square}^{90^\circ}$, we have $\gamma = 1, 2$, $\{\tau^\gamma\} = \{\tau^1, \tau^2\} = \{\tau^x, \tau^y\}$ and $\{\boldsymbol{e}_\gamma\} = \{\boldsymbol{e}_1, \boldsymbol{e}_2\} = \{\boldsymbol{e}_x, \boldsymbol{e}_y\}$.
This generalized notation allows for different compass models and the more well-known models such as the Ising or Heisenberg model to be cast in the same form, see Table 1. For instance the two-dimensional square-lattice Ising model $H_{\square}^{Ising}$ corresponds to $\gamma = 1, 2$ with $\{\tau^\gamma\} = \{\tau^x, \tau^x\}$ and $\{\boldsymbol{e}_\gamma\} = \{\boldsymbol{e}_x, \boldsymbol{e}_y\}$. The Ising model on a three dimensional cubic lattice is then given by $\gamma = 1...3$, $\{\tau^\gamma\} = \{\tau^x, \tau^x, \tau^x\}$ and $\{\boldsymbol{e}_\gamma\} = \{\boldsymbol{e}_x, \boldsymbol{e}_y, \boldsymbol{e}_z\}$. The XY model on a square lattice $H_{\square}^{XY}$ corresponds to $\gamma = 1...4$, $\{\tau^\gamma\} = \{\tau^x, \tau^y, \tau^x, \tau^y\}$ and $\{\boldsymbol{e}_\gamma\} = \{\boldsymbol{e}_x, \boldsymbol{e}_x, \boldsymbol{e}_y, \boldsymbol{e}_y\}$. Another example is the square lattice Heisenberg model, where we have $\gamma = 1...6$, $\{\tau^\gamma\} = \{\tau^x, \tau^y, \tau^z, \tau^x, \tau^y, \tau^z\}$ and $\{\boldsymbol{e}_\gamma\} = \{\boldsymbol{e}_x, \boldsymbol{e}_x, \boldsymbol{e}_x, \boldsymbol{e}_y, \boldsymbol{e}_y, \boldsymbol{e}_y\}$, so that in this case $\sum_\gamma \tau_{\boldsymbol{r}}^\gamma \tau_{\boldsymbol{r}+\boldsymbol{e}_\gamma}^\gamma$ is equal to $\sum_\gamma \boldsymbol{\tau}_{\boldsymbol{r}} \cdot \boldsymbol{\tau}_{\boldsymbol{r}+\boldsymbol{e}_\gamma}$.
This class of compass models can be further generalized in a straightforward manner by allowing for a coupling strength J_γ between the pseudospins τ^γ that depends on the direction of the bond γ (*anisotropic compass models* [6]) and by adding a field h_γ that couples to τ^γ linearly [7, 8]. This generalized class of compass models is then defined by the Hamiltonian

$$\mathcal{H}_{compass} = -\sum_{\boldsymbol{r},\gamma} \left(J_\gamma \tau_{\boldsymbol{r}}^\gamma \tau_{\boldsymbol{r}+\boldsymbol{e}_\gamma}^\gamma + h_\gamma \tau_{\boldsymbol{r}}^\gamma \right). \tag{4}$$

From a historical (as well as somewhat practical) viewpoint the *three dimensional 90° compass model* is particularly interesting. Denoted by $H_{3\square}^{90^\circ}$, it is customarily defined on a cubic lattice and given by $\mathcal{H}_{compass}$, Eq. (4), where γ spans three Cartesian directions: $\gamma = 1, 2, 3$ with $\{\tau^\gamma\} = \{\tau^x, \tau^y, \tau^y\}$, $J_\gamma = J = 1$, $h_\gamma = 0$ and $\{\boldsymbol{e}_\gamma\} = \{\boldsymbol{e}_x, \boldsymbol{e}_y, \boldsymbol{e}_z\}$, so that

$$H_{3\square}^{90^\circ} = -J \sum_{\boldsymbol{r}} \left(\tau_{\boldsymbol{r}}^x \tau_{\boldsymbol{r}+\boldsymbol{e}_x}^x + \tau_{\boldsymbol{r}}^y \tau_{\boldsymbol{r}+\boldsymbol{e}_y}^y + \tau_{\boldsymbol{r}}^z \tau_{\boldsymbol{r}+\boldsymbol{e}_z}^z \right). \tag{5}$$

Thus, by allowing γ to assume values $\gamma = 1, 2, 3$, the square lattice 90 degree compass model of Eq. (3) is trivially extended to three spatial dimensions. Similarly, by allowing $\gamma = 1, 2, ..., D$,

Model Hamiltonian: $\mathcal{H} = -\sum_{\boldsymbol{r},\gamma} \tau^{\gamma}_{\boldsymbol{r}} \tau^{\gamma}_{\boldsymbol{r}+\boldsymbol{e}_\gamma}$

$\{\tau^\gamma\}$	$\{\boldsymbol{e}_\gamma\}$	model name	symbol	dim
$\{\tau^x\}$	$\{\boldsymbol{e}_x\}$	Ising chain	H_1^{Ising}	1
$\{\tau^x, \tau^y\}$	$\{\boldsymbol{e}_x, \boldsymbol{e}_x\}$	XY chain	H_1^{XY}	1
$\{\tau^x, \tau^y, \tau^z\}$	$\{\boldsymbol{e}_x, \boldsymbol{e}_x, \boldsymbol{e}_x\}$	Heisenberg chain	H_1^{Heis}	1
$\{\tau^x, \tau^x\}$	$\{\boldsymbol{e}_x, \boldsymbol{e}_y\}$	square Ising	$H_\square^{Ising}$	2
$\{\tau^x, \tau^x, \tau^x\}$	$\{\boldsymbol{e}_x, \boldsymbol{e}_y, \boldsymbol{e}_z\}$	cubic Ising	$H_{3\square}^{Ising}$	3
$\{\tau^x, \tau^y, \tau^x, \tau^y\}$	$\{\boldsymbol{e}_x, \boldsymbol{e}_x, \boldsymbol{e}_y, \boldsymbol{e}_y\}$	square XY	$H_\square^{XY}$	2
$\{\tau^x, \tau^y, \tau^z, \tau^x, \tau^y, \tau^z\}$	$\{\boldsymbol{e}_x, \boldsymbol{e}_x, \boldsymbol{e}_x, \boldsymbol{e}_y, \boldsymbol{e}_y, \boldsymbol{e}_y\}$	square Heisenberg	$H_\square^{Heis}$	2
$\{\tau^x, \tau^y\}$	$\{\boldsymbol{e}_x, \boldsymbol{e}_y\}$	square 90° compass	$H_\square^{90^\circ}$	2
$\{\tau^x, \tau^y, \tau^z\}$	$\{\boldsymbol{e}_x, \boldsymbol{e}_y, \boldsymbol{e}_z\}$	cubic 90° compass	$H_{3\square}^{90^\circ}$	3
$\{\frac{\tau^x+\sqrt{3}\tau^y}{2}, \frac{\tau^x-\sqrt{3}\tau^y}{2}\}$	$\{\boldsymbol{e}_x, \boldsymbol{e}_y\}$	square 120° compass	$H_\square^{120^\circ}$	2
With $\{\theta_\gamma\} = \{0, 2\pi/3, 4\pi/3\}$:				
$\{\tau^x, \tau^x, \tau^x\}$	$\boldsymbol{e}_x \cos\theta_\gamma + \boldsymbol{e}_y \sin\theta_\gamma$	honeycomb Ising	$H_\hexagon^{Ising}$	2
$\{\tau^x, \tau^y, \tau^z\}$	$\boldsymbol{e}_x \cos\theta_\gamma + \boldsymbol{e}_y \sin\theta_\gamma$	honeycomb Kitaev	$H_\hexagon^{Kitaev}$	2
$\{\tau^x, \tau^x, \tau^z\}$	$\boldsymbol{e}_x \cos\theta_\gamma + \boldsymbol{e}_y \sin\theta_\gamma$	honeycomb XXZ	$H_\hexagon^{XXZ}$	2
$\pi^\gamma = \tau^x \cos\theta_\gamma + \tau^y \sin\theta_\gamma$	$\{\boldsymbol{e}_x, \boldsymbol{e}_y, \boldsymbol{e}_z\}$	cubic 120°	$H_{3\square}^{120^\circ}$	3
π^γ	$\boldsymbol{e}_x \cos\theta_\gamma + \boldsymbol{e}_y \sin\theta_\gamma$	honeycomb 120°	$H_\hexagon^{120^\circ}$	2
With $\{\theta_\gamma\} = \{0, 2\pi/3, 4\pi/3\}$ and $\eta = \pm 1$:				
$\{\tau^x, \tau^y, \tau^z\}$	$\eta\boldsymbol{e}_x \cos\frac{\theta_\gamma}{2} + \eta\boldsymbol{e}_y \sin\frac{\theta_\gamma}{2}$	triangular Kitaev	$H_\triangle^{Kitaev}$	2
π^γ	$\eta\boldsymbol{e}_x \cos\frac{\theta_\gamma}{2} + \eta\boldsymbol{e}_y \sin\frac{\theta_\gamma}{2}$	triangular 120°	$H_\triangle^{120}$	2

Table 1: *Generalized notation that casts compass models and the more well-known model Hamiltonians such as the Ising, XY or Heisenberg models in the same form. Additional spatial anisotropies can be introduced, for instance by coupling constants J_γ that depend on the bond direction $\boldsymbol{e}_\gamma$. Doing so would change the* strengths *of the interaction on different links, but not the form of those interactions: these are determined by how different vector components of $\boldsymbol{\tau}_{\boldsymbol{r}}$ and $\boldsymbol{\tau}_{\boldsymbol{r}+\boldsymbol{e}_\gamma}$ couple.*

it can be extended to arbitrary spatial dimension D (which we will return to in later sections). The structure of $H_{3\square}^{90^\circ}$ is schematically indicated in Fig. 1. This compass model is actually the one that was originally proposed by [1] in the context of orbital ordering. At that time it was noted that even if the interaction on each individual bond is Ising-like, the overall symmetry of the model is considerably more complicated.

It is typical for compass models that even the ground state structure is non-trivial. For a system governed by $H_{3\square}^{90^\circ}$, pairs of pseudospins on lattice links parallel to the x-axis, for instance, favor pointing their pseudospins $\boldsymbol{\tau}$ along x so that the expectation value $\langle \tau^x \rangle \neq 0$, see Fig. 1. Similarly,

on bonds parallel to the y-direction, it is advantageous for the pseudospins to align along the y direction, so that $\langle \tau^y \rangle \neq 0$. It is clear that at any given site the bonds along x, y and z cannot be satisfied at the same time. Therefore the interactions are strongly frustrated. This situation bears resemblance with the dipole-dipole interactions between magnetic needles that are positioned on a lattice, hence the name *compass* models.

Such a frustration of interactions is typical of compass models, but of course also appears in numerous other systems. Indeed, on a conceptual level, many of the ideas and results that will be discussed, such as renditions of thermal and quantum fluctuation-driven ordering effects, unusual symmetries and ground state sectors labeled by topological invariants, have similar incarnations in frustrated spin, charge, cold atom and Josephson junction array systems. Although these similarities are mostly conceptual there are also instances where there are exact correspondences. For instance, the two dimensional 90° compass model is, in fact, dual to the Xu-Moore model describing Josephson coupling between superconducting grains in a square lattice [9–11, 6, 12].

2 Global, topological, and intermediate symmetries and invariances

In terms of symmetries, compass systems are particularly rich. In what follows, we will discuss the invariances that these systems exhibit, but first recall the classification of orders and their relation to symmetry:

(i) *Global symmetry*. In many condensed matter systems (e.g. ferromagnets, liquids), there is an invariance of the basic interactions with respect to global symmetry operations (e.g., continuous rotations in the case of ferromagnets, uniform translations and rotations in liquids) that are to be simultaneously performed on all of the constituents of the system. At sufficiently low temperatures (or strong enough interactions), such symmetries might be *spontaneously* broken.

(ii) *Topological invariants and orders*. Topological orders have been the object of some fascination in more recent years [13]. In the condensed matter community, part of the activity in analyzing these types of order is stimulated by the prospects of fault-tolerant quantum computation. What lies at the crux of topological order is the observation is that even if, in some cases, global symmetry breaking cannot occur, systems may nevertheless still exhibit a robust order of a non-local, topological, type.

The most prominent examples of topological order – long studied by high energy theorists – are afforded by gauge theories [14, 15, 13]. Some of the current heavily studied quintessential models of topological quantum order in condensed matter and quantum information lattice theories, e.g., [16, 13] share much in common with the early pioneering lattice gauge theory concept along with the explicit simplest lattice gauge model first introduced by Franz Wegner [14].

Gauge theories display *local gauge symmetries* and indeed, in pure gauge theories – theories that have only gauge bosons yet no matter sources – the only measurable quantities pertain to correlators defined on loops, the so-called *Wilson loops*. Related products pertain to open contours in some cases when matter sources are present [15, 17, 18].

(iii) *Intermediate symmetry*. The crucial point is that many compass systems display symmetries which, generally, lie midway between the above two extremes of global symmetries and local gauge symmetries. These symmetries are sometimes known as "sliding" symmetries and aside from compass models are also present in numerous other systems. These include, amongst many others, arrays of Luttinger liquids [19, 20], quantum Hall smectic phases [21, 22], ring exchange models of frustrated models [23], and Kondo lattice systems [24]. In the past few years, there been an extremely intense resurgence of interest in such (in particular, "higher-form" type) symmetries that has been triggered anew by their study in the high energy community [25].

To clarify the distinction between these different symmetries, we can rephrase it in a formal way as it applies to general systems [26, 27]. Consider a theory with fields $\{\phi_{\boldsymbol{i}}\}$ that is characterized by a Hamiltonian H (or action $\mathcal{S}$).

Definition: A *d-dimensional gauge-like symmetry* of a theory is a group of symmetry transformations such that the minimal non-empty set of fields $\{\phi_{\boldsymbol{i}}\}$ changed by the group operations occupies a d-dimensional subset ($\mathcal{C}$) of the full D-dimensional region on which the theory is defined. In the following we will refer to such symmetries as *d-dimensional symmetries*.

To exercise this notion it is useful to make contact with known cases. Clearly local gauge symmetries correspond to symmetries of dimension $d = 0$. That is, gauge transformations can be applied locally at any point in space – a region of dimension $d = 0$. At the opposite extreme, e.g., in a nearest neighbor ferromagnet on a D-dimensional lattice, described by the Heisenberg Hamiltonian $H = -J \sum_{\langle ij \rangle} \boldsymbol{S}_i \cdot \boldsymbol{S}_j$, the system is invariant under a global rotation of all spins. As the volume influenced by the symmetry operation occupies a D-dimensional region and in this case $d = D$.

In their simplest form, one which typically appears in compass models, d-dimensional symmetries are of the form

$$\prod_{j \in P} g_j \tag{6}$$

where g_j are group elements associated with a site j and P is a d-dimensional spatial region. In many cases, depending on the boundary conditions of the system, P correspond to entire open d-dimensional planes (as in 90° compass models; see, e.g., Fig. 2) or closed contours (when compass models are endowed with periodic boundary conditions). Defect creation operators (those that restore symmetries) and translations of defects are typically products of local group elements that do not span such an entire region P but rather a fragment of it (see, e.g., the open finite string in Fig. 2 with domain wall boundaries) generally leading to defects at the boundaries where the group element operations are applied [28].

2.1 Exact and emergent symmetries

A Hamiltonian H, and by extension the system it describes, can have two principal kinds of symmetries: exact and emergent ones. These are defined as follows.

(i) *Exact symmetries*. By this, one refers to the existence operators $\hat{O}$ that commute with the

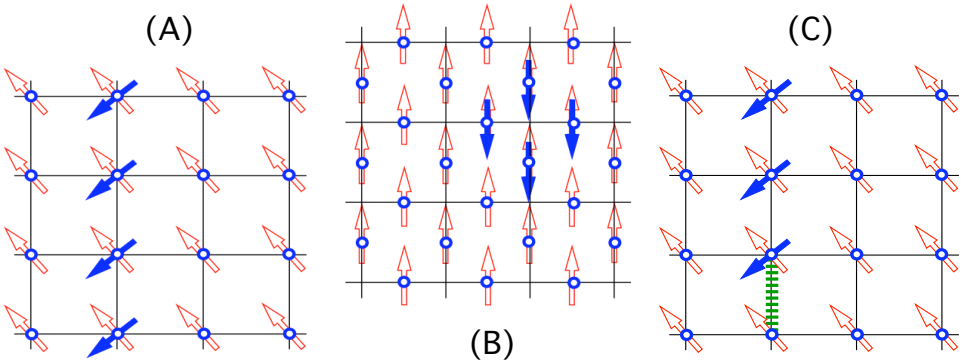

Fig. 2: *(A) The 90° square lattice compass model. The action of the $d = 1$ symmetry operation of Eq. (16) when the "plane" P is chosen to lie along the vertical axis. (B) A $d = 0$ (local) gauge symmetry. Defects within a gauge theory cost a finite amount of energy. Local symmetries such as the one depicted above for an Ising lattice gauge theory cannot be broken. (C) A defect in a semi-classical ground state of the two dimensional orbital compass model. Defects such as this do not allow for a finite on-site magnetization. The energy penalty for this defect is finite (there is only one bad bond – the dashed line) whereas, precisely as in $d = 1$ Ising systems, the entropy associated with such defects is monotonically increasing in system size [28].*

Hamiltonian

$$\left[H, \hat{O}\right] = 0. \tag{7}$$

Such operators, indicated by a hat, $\hat{}$, reflect symmetries of the Hamiltonian.
(ii) *Emergent symmetries*. In many compass (and numerous other) systems, there are operators $\tilde{O}$ that do not commute with the Hamiltonian,

$$\left[H, \tilde{O}\right] \neq 0 \tag{8}$$

i.e., do not satisfy Eq. (7) and are therefore indicated by a tilde, $\tilde{}$. Yet these operators do become symmetries when projected to a particular sector – a particular subset of states on which the Hamiltonian acts. That is,

$$[H, \mathcal{P}\tilde{O}\mathcal{P}] = 0, \tag{9}$$

where $\mathcal{P}$ is the relevant projection operator to that sector. In this case, if one defines $\mathcal{P}\tilde{O}\mathcal{P} = \hat{O}$ then $\hat{O}$ will be an exact symmetry satisfying Eq. (7).
The most prominent cases in condensed matter systems, including compass models in particular (yet also many others, e.g., [24, 29, 30]) relate to symmetries that appear in the *ground state sector* alone. In such instances, the symmetries are sometimes said to *emerge* in the low energy sector of the theory.
Although the formulation above is for quantum Hamiltonians, the same can, of course, be said for classical systems. There are numerous classical systems in which the application of a particular operation on an initial configuration will yield, in general, a new configuration with a differing energy. However, when such an operation is performed on a particular subset of configurations, such as the classical ground states, it will lead to other configurations that have precisely the same energy as the initial state. Similarly, certain quantum systems exhibit such particular symmetries

only in their large pseudo-spin (or classical) limit. In such cases, symmetries may be said to emerge in the large pseudo-spin (or classical) limit.

One should note that emergent low-energy symmetries are notably different from the far more standard situation of spontaneous symmetry breaking, wherein an invariance of the Hamiltonian (or action) is spontaneously broken in individual low energy states (which are related to one another by the symmetry operation at hand). In the condensed matter arena, the canonical example is rotationally symmetric ferromagnets in a spatial dimension larger than two, in which at sufficiently low temperature a finite magnetization points along a certain direction – thus breaking the rotational symmetry. Another canonical example is the discrete (*up* $\leftrightarrow$ *down* or) time reversal symmetry which is broken in Ising ferromagnets in dimensions large than one. Spontaneous symmetry breaking appears in systems that exhibit long-range order of some sort such as crystallization (breaking translational and rotational symmetries), superconductors (local gauge invariance and a Anderson-Higgs mechanism), or superfluid Helium. Other examples include the Higgs mechanism of particle physics, chiral symmetry breaking in quantum chromodynamics, nucleon pairing in nuclei, electro-weak symmetry breaking at low energies, and related mass generation.

In all of these textbook examples, the system is symmetric at high energies and exhibits low-energy states that do not have that symmetry. However, in low energy emergent symmetries, the situation is reversed: the system may become *more* symmetric in the low-energy sector. We will discuss explicit examples of exact and emergent symmetries in compass models in the following sections.

2.2 Consequences of intermediate symmetry

2.2.1 Degeneracy of spectrum

We now briefly discuss how the presence of a d-dimensional intermediate symmetry, either classical or quantum, implies an exponential degeneracy of the energy spectrum that corresponds to the Hamiltonian. The application of intermediate symmetries on disparate d-dimensional planes leads to inequivalent states that all share the same energy. If a symmetry transformation $\tilde{O}_P$ has its support on a d-dimensional plane P, then one can define the composite symmetry operators

$$\tilde{O}_{composite} = \tilde{O}_{P_1}\tilde{O}_{P_2}..\tilde{O}_{P_R}. \tag{10}$$

For a hypercubic lattice in D dimensions which is of size $L\times L\times L\cdots\times L$, the number of independent planes (R) in Eq. (10) scales as $R = \mathcal{O}(L^{d'})$ where

$$d' = D - d. \tag{11}$$

If each individual d-dimensional symmetry operation (exact or emergent) U_{P_i} leads to a degeneracy factor of m then the composite operation of Eq. (10) can lead to a degeneracy (of any state (for exact symmetries) or of the ground state (for emergent symmetries)) whose logarithm is of magnitude

$$\log_m \mathsf{degeneracy} = \mathcal{O}(L^{D-d}). \tag{12}$$

That this is indeed the case is clearer for classical systems with discrete symmetries than for quantum systems. Nevertheless, in the thermodynamic limit and/or on lattices whose boundaries are tilted the degeneracy factor of Eq. (12) associated with the intermediate d-dimensional symmetries becomes exact [31]. On hypercubic lattices, such as the square lattice of the planar 90° compass model discussed in subsection 2.3, whose boundaries are the same along the d' directions orthogonal to the planes P, the application of the operators of Eq. (10) does not lead to independent states for finite size systems. However, in the thermodynamic limit, the application of disparate operators of the form of Eq. (10) on a given initial state may lead to orthogonal states.

2.2.2 Dimensional reduction

The existence of intermediate symmetries has important consequences: it implies a dimensional reduction. The corresponding dimensional reduction is only with respect to expectation values of local quantities: the free energies of these systems and the transitions that they exhibit are generally those of systems in high dimensions [26, 27].

Theorem on Dimensional Reduction More precisely, the expectation value of any such quantity $\langle f \rangle$ in the original system (of dimension D) is bounded from above by the expectation value of the same quantity evaluated on a d dimensional region:

$$|\langle f \rangle| \leq |\langle f \rangle|_{H_d}. \tag{13}$$

The expectation value $\langle f \rangle$ refers to that done in the original system (or lattice) that resides in D spatial dimensions. The Hamiltonian H_d on the right-hand side is defined on a d dimensional subregion of the full lattice (system). The dimensionality $d \leq D$. The Hamiltonian H_d preserves the range of the interactions of the original systems. It is formed by pulling out of the full Hamiltonian on the complete (D dimensional) lattice, the parts of the Hamiltonian that appear within the d dimensional sub-region ($\mathcal{C}$) on which the symmetry operates. Fields (spins) external to $\mathcal{C}$ act as non-symmetry breaking external fields in H_d. The bound of Eq. (13) becomes most powerful for quantities that are not symmetry invariant as then the expectation values $\langle f \rangle_{H_d}$ need to vanish for low spatial dimensions d (as no spontaneous symmetry breaking can occur). This, together with Eq. (13), then implies that the expectation value of $\langle f \rangle$ on the full D dimensional spatial lattice must vanish. By "non invariant" we mean that $f(\phi_{\boldsymbol{i}})$ vanishes when summed over all arguments related to each other a d dimensional symmetry operation, $\sum_k f[\boldsymbol{g}_{\boldsymbol{i}k}(\phi_{\boldsymbol{i}})] = 0$. For continuous symmetries, non-invariance explicitly translates into an integral over the group elements $\int f[\boldsymbol{g}_{\boldsymbol{i}}(\phi_{\boldsymbol{i}})]\, d\boldsymbol{g} = 0$.
We will now summarize general corollaries of such symmetry based analysis for general systems.

Corollaries By choosing f to be the order parameter or a two-particle correlator, one arrives at the following general corollaries [26, 32, 27]:
Corollary I: Any local quantity that is not invariant under local symmetries ($d = 0$) or symmetries that act on one dimensional regions ($d = 1$) has a vanishing expectation value $\langle f \rangle_{H_d}$ at any finite

temperature. This follows as both zero- and one-dimensional systems cannot exhibit symmetry breaking: in one and two dimensional systems, the expectation value of any local quantities not invariant under global symmetries: $\langle f \rangle = 0$.

Physically, entropy overwhelms energetic penalties and forbids a symmetry breaking. Just as in zero- and one-dimensional systems, much more entropy is gained by introducing defects (e.g., domain walls in discrete systems), the same energy-entropy calculus is replicated when these symmetries are embedded in higher dimensions. An example with $d = 1$ domain walls in a two-dimensional systems is afforded by the planar 90° compass model (see Fig. 2); even though the planar compass model is two-dimensional, the energy cost of these domain walls is identical to that in a $d = 1$ system. The particular case of local ($d = 0$) symmetry is that of Elitzur's theorem [33] so well known in gauge theories. We may see it more generally as a consequence of dimensional reduction.

A discussion of how, by virtue of this consequence, such symmetries may protect and lead to topological quantum orders in systems at both finite and zero temperature appears in [34, 28].

Corollary II: One can push the consequences further by recalling that no symmetry breaking occurs for continuous symmetries in two spatial dimensions. Here again, free energy penalties are not sufficiently strong to induce order. When embedding continuous two dimensional symmetries in higher dimensions, the energy entropy balance is the same and the same result is attained $\langle f \rangle = 0$ at all finite temperatures for any quantity f that is not invariant under continuous $d \leq 2$ symmetries.

Further noting that order does not exist in continuous two dimensional systems also at zero temperature in the presence of a gap between ground and the next excited state, one similarly finds that for a $d \leq 2$ dimensional continuous symmetry the expectation value of any local quantity not invariant under this symmetry, strictly vanishes at zero temperature. Though local order cannot appear, multi-particle (including topological) order can exist. In standard gauge ($d = 0$) theories, the product of gauge degrees of freedom along a closed loop (the Wilson loop) can attain a non-zero value as it may be invariant under all $d = 0$ symmetries. In more general theories with higher d dimensional symmetries, similar considerations may lead to loop (or "brane") type correlators that involve multiple fields and are invariant under all low dimensional symmetries. Precisely such non-local correlation functions appear in Kitaev's honeycomb model and many other systems with topological orders [35, 28, 34, 36]. Symmetry breaking in the highly degenerate compass models often transpires by a fluctuation driven mechanism ("order by disorder") [37–39]. In this mechanism, entropic contributions to the free energy play a key role.

Corollary III: Not only can one make statements about the absence of symmetry breaking, we can also adduce fractionalization of non-symmetry invariant quantities in high dimensional system. That occurs if no (quasi-particle type) resonant terms appear in the lower dimensional spectral functions [32].

This corollary allows for fractionalization in quantum systems, where $d = 1, 2$. It enables symmetry invariant quasi-particles excitations to *coexist* with non-symmetry invariant fractionalized excitations. Fractionalized excitations may propagate in $D-d$ dimensional regions. Examples afforded by several frustrated spin models where spinons may drift along lines on the square

lattice [29] and in D dimensional regions on the pyrochlore lattice [30].
In what follows, we explicitly enumerate the symmetries that appear in various compass models. The *physical origin of dimensional reduction* in these systems can be seen examining intermediate symmetry restoring defects.

2.3 Symmetries of the 90° compass model

We now classify symmetries of the 90° compass model in various spatial dimensions, considering both quantum and classical versions. To highlight some aspects of the symmetries of this system, it is profitable to discuss the general anisotropic compass model, as given for $D = 2$ in Eq. (1) with general couplings J_x and J_y and in general spatial dimension D given by Eq. (4), without field

$$H_{D\square}^{90^\circ} = -\sum_{\boldsymbol{r},\gamma} J_\gamma \, \tau_{\boldsymbol{r}}^\gamma \tau_{\boldsymbol{r}+\boldsymbol{e}_\gamma}^\gamma \, . \tag{14}$$

The equivalent classical Hamiltonian on a D-dimensional hyper cubic lattice is

$$H_{D\square}^{90^\circ,\,\text{class}} = -\sum_{\boldsymbol{r},\gamma} J_\gamma \, T_{\boldsymbol{r}}^\gamma T_{\boldsymbol{r}+\boldsymbol{e}_\gamma}^\gamma \, . \tag{15}$$

In the quantum systems, T^γ are generators of the representations of SU(2) of size $(2T+1)$. For a pseudo-spin 1/2 system, $T^\gamma = \tau^\gamma/2$. In the classical arena, T^γ are the Cartesian components of normalized vector $\boldsymbol{T}$. These classical and quantum Hamiltonian systems exhibit both exact and emergent symmetries.

2.3.1 Exact discrete intermediate symmetries

Exact symmetries of both the square lattice and cubic lattice 90° compass model in any pseudo-spin representation are given by [26, 40–42, 6, 43]

$$\hat{O}^{(\gamma)} = \prod_{\boldsymbol{r}\in P_\gamma} e^{i\pi T_{\boldsymbol{r}}^\gamma} \tag{16}$$

where P_γ is any line (in the case of the two-dimensional model) or plane (in the case of the cubic lattice model) which is orthogonal to the external $\boldsymbol{e}_\gamma$ axis of the lattice. A schematic for the $D = 2$ dimensional case is provided in panel (a) of Fig. 2.
The exact nature of the symmetries of Eq. (16) is readily seen: the operators of Eq. (16) commute with the general Hamiltonian of Eq. (15): $[O^{(\gamma)},\, H] = 0$. Thus, rotations of individual planes about an orthogonal axis leave the system invariant. Written generally, for a 90° compass model in D dimensions, the planes P_γ are objects of spatial dimensionality $d = D-1$. In the $D = 3$ dimensional system, the symmetries of Eq. (16) are of dimension $d = 2$ as the planes P_γ are two-dimensional objects. On the square lattice, the symmetries are of dimension $d = 1$ as P_γ are lines. These symmetries hold for both the quantum system with arbitrary size pseudo-spin as well as the classical system in a high number of dimensions D. A consequence of these symmetries is an exponential in L^{D-1} degeneracy of each eigenstate of the Hamiltonian (including but

not limited to ground states) in systems with "tilted" boundary conditions that emulate the thermodynamic limit [31]. In pseudo-spin one-half realizations of this system, Eq. (14), on an $L \times L$ square lattice, a 2^L degeneracy was numerically adduced for anisotropic systems ($J_x \neq J_y$) in the thermodynamic limit [43]. Correlation functions involving the symmetry operators were examined in [44].

Now, here is an important point to which we wish to reiterate – that of the *physical origin of the dimensional reduction in this system.* In a $D = 2$ dimensional 90° compass model system, the energy cost for creating defects (domain walls) is identical to that in a $d = 1$ dimensional system (see Fig. 2). With the aid of the bound of Eq. (13), we then see the finite temperature expectation value $\langle \sigma_i^z \rangle = 0$ within the $D = 2$ orbital compass model. The physical engine behind the loss of on-site order of $\langle \sigma_i^z \rangle$ is the proliferation of solitons, see Fig. 2. Just as in $d = 1$ dimensional systems, domain walls (solitons) cost only a finite amount of energy while their entropy increases with system size. A schematic is provided in panel (c) of Fig. 2. The Hamiltonian $H_{d=1}$ defined on the vertical chain of Fig. 2 where these operations appear is none other than a one dimensional Ising Hamiltonian augmented by transverse fields generated by spins outside the vertical chain. Any fixed values of the spins outside the $d = 1$ dimensional chain lead to transverse fields that act on the chain. These along the Ising exchange interactions between neighboring spins along the chain lead in this case to the pertinent $H_{d=1}$ in Eq. (13): that of a transverse field Ising model Hamiltonian. By virtue of their location outside the region where the symmetry of Eq. (16) operates, the spins $\sigma^x_{i \notin P_x}$ do not break the discrete $d = 1$ symmetry associated with the plane P_x. These defects do not enable a finite temperature symmetry breaking.

2.3.2 Exact discrete global symmetries

When the couplings are not completely anisotropic (e.g., $J_x = J_y \neq J_z$ or $J_x = J_y = J_z$ on the cubic lattice or $J_x = J_y$ on the square lattice) there are additional discrete symmetries augmenting the $d = D-1$ Ising symmetries detailed above. For instance, when $J_x = J_y \neq J_z$ a global discrete rotation of all pseudo-spins on the lattice by an angle of 90° about the T^z direction leaves the Hamiltonian of Eq. (15) invariant. Such a discrete rotation essentially permutes the x and y oriented bonds which are all of equal weight in the isotropic case when these are summed over the entire square lattice. The same, of course, also applies for the square lattice model when $J_x = J_y$.

Yet another possible representation of essentially the same symmetry as it is pertinent to the exchange of couplings in the compass model is that of a uniform global rotation by 180° about the $(1, 1)/\sqrt{2}$ direction of the pseudo-spins. Similarly, when $J_x = J_y = J_z$, a uniform global rotation by 120° of all pseudo-spins about the internal $(1, 1, 1)/\sqrt{3}$ pseudo-spin direction is also a discrete symmetry; this latter symmetry is of the Z_3 type – if performed three times in a row, this will give back the identity operation.

These additional discrete symmetries endow the system with a higher degeneracy. For isotropic systems ($J_x = J_y$), numerically a 2^{L+1} fold degeneracy is seen in the pseudo-spin $T = 1/2$ system [43]; this additional doubling of the degeneracy is related to a global Ising operation of a

rotation by 180° about a chosen pseudo-spin direction that leaves the system invariant. These additional symmetries are global symmetries and thus of a dimension $d = D$ which is higher than that of the discrete lower dimensional that are present in both the anisotropic and isotropic systems ($d = D-1$). As a result, in, e.g., the isotropic $D = 2$ dimensional 90° compass model may exhibit a finite temperature breaking of such a discrete global symmetry associated with such a discrete rotation. By contrast, the $d = 1$ symmetries of the two-dimensional 90° compass model cannot be broken as discussed in section 2.2.2.

We note that in the classical anisotropic rendition of this system the degeneracy is exactly the same – i.e., 2^L, aside from continuous emergent symmetries that will be discussed in the next section. The classical isotropic case is somewhat richer. There, each uniform pseudo-spin state has an additional degeneracy factor of 2^{2L} associated with the $2L$ independent classical $d = 1$ Ising symmetries.

2.3.3 Emergent intermediate discrete symmetries: cubic 90° model

We now turn to intermediate symmetries that appear in the large pseudo-spin (or classical) limit of the 90° compass model in three dimensions. In its classical limit, the 90° compass model on the cubic lattice has $d = 1$ inversion (or reflection) symmetries along lines parallel to each of the three Cartesian axes x_a. Along these lines, we may set $\tau_i^a \to -\tau_i^a$ and not touch the other components. This corresponds to, e.g, a reflection in the internal xy pseudo-spin plane when we invert τ^z and not alter the x or y components.

We explicitly note that this transformation is not canonical and does not satisfy the commutation relation and is thus disallowed quantum mechanically; indeed, this appears only as an emergent symmetry in the classical limit of large pseudo-spin. Instead in the 90° compass model on the cubic lattice, quantum mechanically we have the $d = 2$ symmetries which we wrote earlier (which of course trivially also hold for the classical system). Thus, the quantum system is less symmetric than its classical counterpart.

By contrast to the cubic lattice case, for the square lattice 90° compass model, the intermediate $d = 1$ symmetries of Eq. (16) are are not emergent symmetries but rather exact quantum (as well as classical) symmetries.

2.3.4 Emergent continuous global symmetries

In addition to its exact symmetries, the 90° model also exhibits emergent symmetries in its isotropic version. As mentioned earlier, globally uniform pseudo-vector configurations are ground states of any classical isotropic ferromagnetic compass model. Thus any global rotation of all pseudo-spins is an emergent symmetry of the 90° models. In the $D = 2$ system, this corresponds to a global U(1) rotation of all angles of the planar pseudo-spins. In the $D = 3$ cubic lattice system, any SO(3) rotation of the three-dimensional pseudo-spins is an emergent symmetry. That a rotation does not change the energy of any uniform configuration is clear in the 90° model. Imagine that all pseudo-spins in the planar 90° model are oriented at an angle θ relative to the T^x axis. In such a case, the energy associated with the horizontal bonds,

$T^x_{\boldsymbol{r}} T^x_{\boldsymbol{r}+\boldsymbol{e}_x}$ will vary as $\cos^2\theta$ whereas that associated with the vertical bonds varies as $\sin^2\theta$. As $J_x = J_y = J$ in the isotropic system and as $\sin^2\theta + \cos^2\theta = 1$, any uniform pseudo-spin state will have the same energy and global rotations will not alter this energy.

3 Kitaev's honeycomb model

In 2006, Alexei Kitaev introduced a type of compass model that has interesting topological properties and excitations, which are relevant and much studied in the context of topological quantum computing [45]. The model is defined on a honeycomb lattice and is referred to either as *Kitaev's honeycomb model* or the *XYZ honeycomb compass model*. The lattice links on a honeycomb lattice may point along three different directions, see Fig. 3. One can label the bonds along these directions by $\boldsymbol{e}_1$, $\boldsymbol{e}_2$ and $\boldsymbol{e}_3$, where the angle between the three unit lattice vectors is 120°. With these preliminaries, the Kitaev's honeycomb model Hamiltonian $H^{Kitaev}_{\hexagon}$ reads

$$H^{Kitaev}_{\hexagon} = -J_x \sum_{\boldsymbol{e}_1-\text{bonds}} \tau^x_i \tau^x_j - J_y \sum_{\boldsymbol{e}_2-\text{bonds}} \tau^y_i \tau^y_j - J_z \sum_{\boldsymbol{e}_3-\text{bonds}} \tau^z_i \tau^z_j$$

One can re-express this model in the form of $H_{compass}$ introduced above, where

$$H^{Kitaev}_{\hexagon} = -\sum_{\boldsymbol{r},\gamma} J_\gamma \tau^\gamma_{\boldsymbol{r}} \tau^\gamma_{\boldsymbol{r}+\boldsymbol{e}_\gamma} \qquad \text{with} \qquad \begin{cases} \{\tau^\gamma\} = \{\tau^x, \tau^y, \tau^z\} \\ \{J_\gamma\} = \{J_x, J_y, J_z\} \\ \boldsymbol{e}_\gamma = \boldsymbol{e}_x \cos\theta_\gamma + \boldsymbol{e}_y \sin\theta_\gamma \\ \{\theta_\gamma\} = \{0, 2\pi/3, 4\pi/3\} \end{cases} \tag{17}$$

It was proven that for large J_z, the model Hamiltonian $H^{Kitaev}_{\hexagon}$ maps onto a square lattice model known as *Kitaev's toric code model* [16].

3.1 Features of Kitaev's honeycomb model

By its very nature, Kitaev's honeycomb model is very similar to the 90° compass models and other 120° models [4]. However, the Kitaev-model system has a number of very remarkable properties. These can be assessed in a crisp manner because the model is exactly solvable: it can be mapped exactly onto a system of non-interacting Majorana (as well as Dirac) fermions, as will be detailed in Sec. 3.2.2. This allows the derivation of all of the beautiful topological characteristics – its gapped bulk states, computable Chern numbers and Majorana excitations. Moreover, it will make evident that these Majorana excitations are coupled to a gauge field which embodies the topological charges, i.e., magnetic and electric like charges.
For future purposes it is useful to define an extension to this Hamiltonian $H^h_{\hexagon}$, which actually becomes relevant if the model is studied in an external field h. This term involves three pseudo-spins on sites i, j and k, and is the of form

$$H^h_{\hexagon} = -\kappa \sum_{ijk} \tau^x_i \tau^y_j \tau^z_k \tag{18}$$

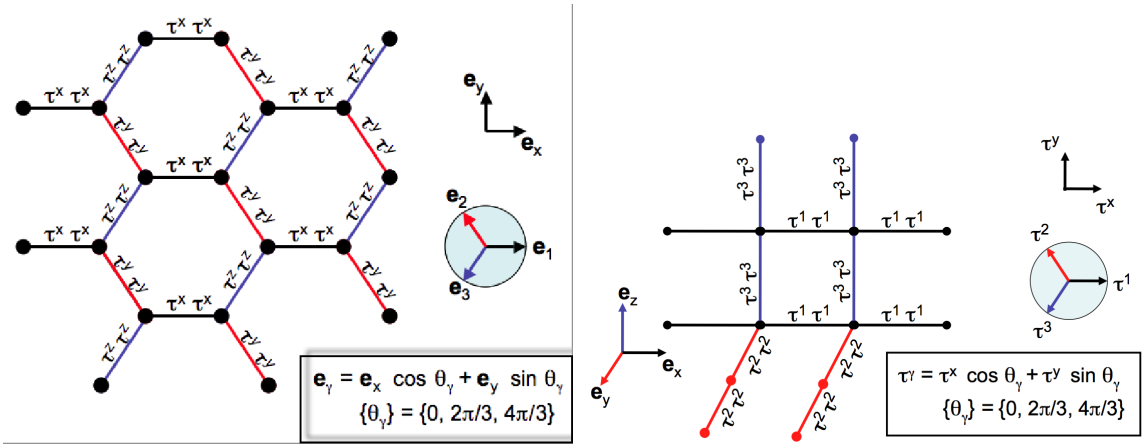

Fig. 3: *Left: Kitaev's compass model on a honeycomb lattice: the interaction of (pseudo-)spin degrees of freedom* $\boldsymbol{\tau} = (\tau^x, \tau^y, \tau^z)$ *along the three bonds that each site is connected to are* $\tau^x_{\boldsymbol{r}}\tau^x_{\boldsymbol{r}+\boldsymbol{e}_1}$, $\tau^y_{\boldsymbol{r}}\tau^y_{\boldsymbol{r}+\boldsymbol{e}_2}$ *and* $\tau^z_{\boldsymbol{r}}\tau^z_{\boldsymbol{r}+\boldsymbol{e}_3}$, *where the bond-vectors of the honeycomb lattice* $\{\boldsymbol{e}_1, \boldsymbol{e}_2, \boldsymbol{e}_3\}$ *are* $\{\boldsymbol{e}_x, (-\boldsymbol{e}_x+\sqrt{3}\boldsymbol{e}_y)/2, (-\boldsymbol{e}_x-\sqrt{3}\boldsymbol{e}_y)/2\}$, *respectively. Right: The 120° compass model on a cubic lattice: the interaction of (pseudo-)spin degrees of freedom* $\boldsymbol{\tau} = (\tau^x, \tau^y, \tau^z)$ *along the three bonds that each site is connected to are* $\hat{\pi}^1_{\boldsymbol{r}}\hat{\pi}^1_{\boldsymbol{r}+\boldsymbol{e}_x}$, $\hat{\pi}^2_{\boldsymbol{r}}\hat{\pi}^2_{\boldsymbol{r}+\boldsymbol{e}_y}$ *and* $\hat{\pi}^3_{\boldsymbol{r}}\hat{\pi}^3_{\boldsymbol{r}+\boldsymbol{e}_z}$, *where the different components* $\{\hat{\pi}^1, \hat{\pi}^2, \hat{\pi}^3\}$ *of the vector* $\hat{\boldsymbol{\pi}} = (\tau^x, (-\tau^x+\sqrt{3}\tau^y)/2, (-\tau^x-\sqrt{3}\tau^y)/2)$ *interact along the different bonds* $\{\boldsymbol{e}_x, \boldsymbol{e}_y, \boldsymbol{e}_z\}$.

where the sum over ijk is a sum over *all* sites connected by the two links $\langle ij\rangle$ and $\langle jk\rangle$. So here the link $\langle ij\rangle$ connects neighboring sites i and j, similarly for $\langle jk\rangle$, but sites i and k are *next* nearest neighbors. This form of the Hamiltonian might seem rather particular at this point, but when adding it, the model will stay exactly solvable. This term is essential in order to endow the non-Abelian excitations of Kitaev's honeycomb model with a gap. The Kitaev model reduces to the *toric code model* in the limit in which one coupling constant is far larger than all of the rest, e.g., $|J_z| \gg |J_{x,y}|$. The excitations in the toric code model, precisely have magnetic and electric charges.

3.1.1 Majorana excitations

The existence of edge-states in the Kitaev model constitutes an analogue to quantum Hall systems and other topological insulators. However, in integer quantum Hall systems, the edge-modes are bona fide fermions and not Majorana fermions. It is the Majorana character of the excitations that in principle enables the aforementioned fault tolerance relative to *all* local fluctuations – "errors" in the setting of quantum computing. The excitations of the Kitaev model flesh out the notions of anyonic statistics and afford very crisp realizations of non-trivial topology. The system also realizes one of the simplest examples of exotic ideas concerning fractionalization in strongly correlated electronic and spin systems. In its Abelian phase, the *magnetic* and *electric* excitations in the model may, respectively, be viewed [47] as counterparts of *vison* and *spinon* excitations in theories of doped quantum antiferromagnets [48] with relative "semionic" statistics which requires that when an excitation of one type is moved around another it picks up a phase factor of -1.

It should be stressed that while the existence of excitations of Majorana-type is a special feature of the Kitaev model, it is not necessarily a unique feature. In special situations three dimensional topological insulators may also exhibit Majorana fermion type of excitations, for instance on their surface when placed at an interface with a superconductor [49]. Majorana fermions may also manifest in some of the systems that we earlier referred to in the context of non-trivial statistics: the fractional quantum Hall systems such that of the state of filling fraction $\nu = 5/2$ [50], at cores of half-vortices in p-wave superconductors [51] and in semi-conductor [52, 53] and semi-conductor/(s-wave) superconductor systems [54].

3.2 Majorana representation – Abelian phases

As was emphasized earlier, the Kitaev model is exactly solvable in its ground state sector, for any set of coupling constants J_x, J_y and J_z. The original solution in [45] hinged on introducing several Majorana fermion degrees of freedom per site and making a projection on to a physical Hilbert space and symmetrization. Later approaches invoked a Jordan-Wigner (JW) transformation in two dimensions [55, 35, 56, 57], perturbative methods, e.g., [58] and slave fermion methods [59, 60]. Another approach, which will be followed here, is based on the direct use of a *bond algebra* [61]. It is rather straightforward and keeps directly track of the local symmetries that the Hamiltonian harbors, which are crucial to the solutions of $H^K_{\hexagon}$ (and the same model augmented by $H^h_{\hexagon}$). The explicit solution via the JW transformation [35] largely inspired the bond algebraic approach, but it is not as direct. The advantage of the bond algebraic method is that it enables the solution without enlarging the Hilbert space and making subsequent projections. Nor does it use at intermediate steps non-local string operators as in the Jordan-Wigner transformation.

3.2.1 Bond algebra, symmetries, and anyonic charge

In the Kitaev Hamiltonian $H^K_{\hexagon}$ three types of bonds $\{b_{jk}\}$ appear

$$\tau^x_j \tau^x_{j+\boldsymbol{e}_1},\ \tau^y_j \tau^y_{j+\boldsymbol{e}_2} \text{ and } \tau^z_j \tau^z_{j+\boldsymbol{e}_3}, \tag{19}$$

where $\{\boldsymbol{e}_1, \boldsymbol{e}_2, \boldsymbol{e}_3\}$ are unit vectors along the three directions of the hexagonal lattice. In terms of bond operators the Hamiltonian is

$$H^K_{\hexagon} = \sum_{\langle jk \rangle} J_{jk} b_{jk}, \tag{20}$$

with $J_{jk} = J_x, J_y$ or J_z depending on the orientation of bond $\langle jk \rangle$ along one of the three directions. One usually supplements this definition of the bond-Hamiltonian with an ordering convention of the bonds, the simplest one being that site j always lies below site k in the honeycomb lattice as for instance shown in Fig. 4. The pseudo-spin operators anticommute at any given site j, e.g., $\{\tau^x_j, \tau^z_j\} = 0$, and commute at different sites, e.g., $[\tau^x_j, \tau^z_p] = 0$ for any two sites $j \neq p$. The bonds therefore satisfy an extraordinarily simple algebra [61]:

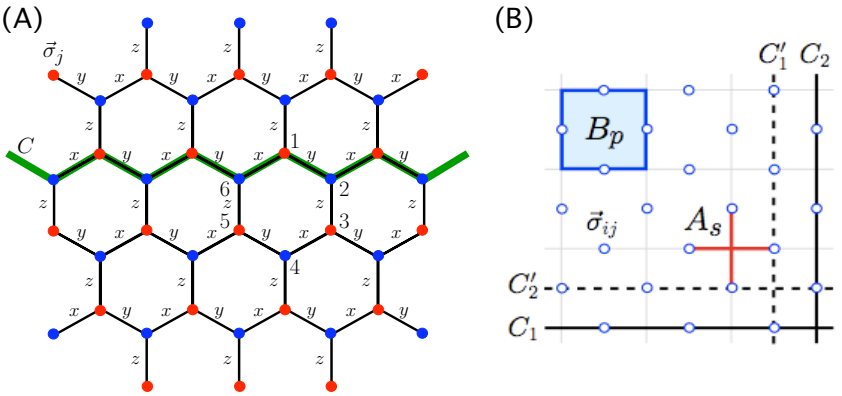

Fig. 4: *(A) Kitaev's model on a honeycomb lattice and three types of bonds. On each vertex there is an $S = 1/2$ degree of freedom indicated by a Pauli matrix $\vec{\sigma}_j$ (see text). (B) Elementary plaquette B_p and star A_s interaction terms in Kitaev's Toric code model. Hollow circles in the bonds (links) represent an $S = 1/2$ degree of freedom, while thick (dashed or solid) lines represent topological ($d = 1$) symmetry operators (see text). [46]*

(i) The square of each bond is one.

(ii) Two bonds that do not share any common site commute.

(iii) Two bonds that share one common site anti-commute.

There are no additional algebraic relations that the bonds that appear in the Hamiltonian $H^K_{\hexagon}$ need to satisfy. This set of all algebraic relations between the bonds in a general Hamiltonian is termed the *bond algebra* [12, 62, 7]. If we can write down another representation of the bonds in Eq. (19) for which all of the above algebraic relations are the same, then the Hamiltonian in the new representation and the original one will share the same spectrum and are thus related by a unitary transformation (and are thus dual to one another). Precisely such a change of representation underlies the exact solution of $H^K_{\hexagon}$ (as further elaborated on in subsections 3.2.2 and 3.2.3). Similar dualities (including those that lead to an effective dimensional reduction) can be established in numerous other compass models, e.g., [63, 64, 12, 62, 7, 65, 66, 34, 27].
We now pause to examine the symmetries of the Hamiltonian $H^K_{\hexagon}$. Exact local ($d = 0$) gauge symmetries are given by *products of pseudo-spins around each hexagon* [45]. For each hexagon i labeled by $\hexagon i$ as in Fig. 5, such a symmetry is given by

$$\hat{O}_{\hexagon i} = \tau_1^z \tau_2^x \tau_3^y \tau_4^z \tau_5^x \tau_6^y . \tag{21}$$

These local symmetries are *Ising gauge* symmetries (the square of these symmetry operators is identically equal to one and all of the symmetry operators for different hexagons commute with one another).
Each of the six sites of the hexagon contributes only one component τ^γ of its pseudo-spin operator to the product $\hat{O}_{\hexagon i}$, where γ is either x, y or z. Precisely which component of these three depends on the type of link that is *not* part of the hexagon – if on site j the bond operator

on the "non-hexagon link" is of type $\tau_j^\gamma \tau_{j+\boldsymbol{e}}^\gamma$ (thus with $j \in \hexagon i$ and $j+\boldsymbol{e} \notin \hexagon i$), the pseudo-spin component appearing in $\hat{O}_{\hexagon i}$ is τ_j^γ.
It can readily be verified that $\hat{O}_{\hexagon i}$ commutes with *any* bond-operator b_{jk} of Eq. (19) and consequently $[H_{\hexagon}^K, \hat{O}_{\hexagon i}] = 0$. These operators also mutually commute with one another: $[\hat{O}_{\hexagon i}, \hat{O}_{\hexagon j}] = 0$. Moreover the square of each such symmetry operator is one: $\hat{O}_{\hexagon i}^2 = 1$. When it attains a non-trivial eigenvalue, i.e., $\hat{O}_{\hexagon i} = -1$, the operator $\hat{O}_{\hexagon i}$ is said to depict an *anyonic charge* or *vorticity* on hexagon i, for reasons which will become clear later.
From the above follows that the system is composed of 2^{N_h} sectors with $N_h = N/2$ being the number of hexagons. Each sector is specified by the set of eigenvalues of the operators $\{\hat{O}_{\hexagon i}\}$, where $i = 1, ..., N_h$: $|O_{\hexagon 1} = \pm 1, O_{\hexagon 2} = \pm 1, ..., O_{\hexagon N_h} \pm 1\rangle$.
The model has more symmetries. When the system is placed on a torus, $H_{\hexagon}^K$ also has $d = 1$ symmetries, using the classification of symmetries of Section 2. For any loop C that spans the entire system the symmetry given by $\prod_{j \in C} \tau_j^\gamma$, where on each site j the component γ is determined by the character of one bond of site j that is not on C (i.e., the bond $\tau_j^\gamma \tau_{j+\boldsymbol{e}}^\gamma$ with $j \in C$ and $j+\boldsymbol{e} \notin C$). When C is for instance taken to be the zig-zag contour shown in Fig. 4 this symmetry is $\prod_{j \in C} \tau_j^z$, but actually any *closed* loop C represents a symmetry.

3.2.2 Majorana representation and fermionization

The relations (i)-(iii) of the previous section define the bond algebra of $H_{\hexagon}^K$ and it can readily be checked that they are also satisfied by the following substitution for the bonds in Eq. (19):

$$b_{jk} = 2i\eta_{jk} c_j c_k, \tag{22}$$

where the operators c_j represent *Majorana fermions*, obeying the Majorana algebra and η_{jk} are Ising-type gauge links: a number that is either $+1$ or -1 on any given link $\langle jk \rangle$. Since the Majorana fermions anticommute, we will choose the ordering convention such that the site j always lies below k. The set $\{\eta_{jk}\}$ encompassing all bonds constitutes a sector of gauge links. In any given sector $\{\eta_{jk}\}$, the Hamiltonian of Eq. (20) is quadratic in the Majorana fermions $\{c_i\}$ and *thus exactly solvable* [45, 61]. The local ($d = 0$) symmetries of Eq. (21) can be expressed in terms of the bonds as

$$\hat{O}_{\hexagon i} = \prod_{jk \in \hexagon i} \eta_{jk}. \tag{23}$$

That is, each sector of fixed $\{\eta_{jk}\}$ is an eigenstate of the symmetry operators of Eq. (21) with an eigenvalue that is determined only by $\{\eta_{jk}\}$. In $\hat{O}_{\hexagon i}$, as one multiplies η_{jk} for all links $\langle jk \rangle$ that are in the hexagon i, one keeps the bond indices j and k ordered with the previously chosen convention of j being below k.
The expression for $\hat{O}_{\hexagon i}$ above highlights the similarity between the local gauge symmetries in this system and such general symmetry (and fluxes) elsewhere. For instance, in a lattice version of electromagnetism, Eq. (23) relates to an Aharonov Bohm like phase. In the current context, Eq. (23) relates to the Ising version of such a phase ($O_{\hexagon i} = \pm 1$).
As each site belongs to three hexagons and each hexagon contains six sites, the number of hexagons is half the number of lattice sites ($N_h = N/2$). Thus to account for all eigenvalues of

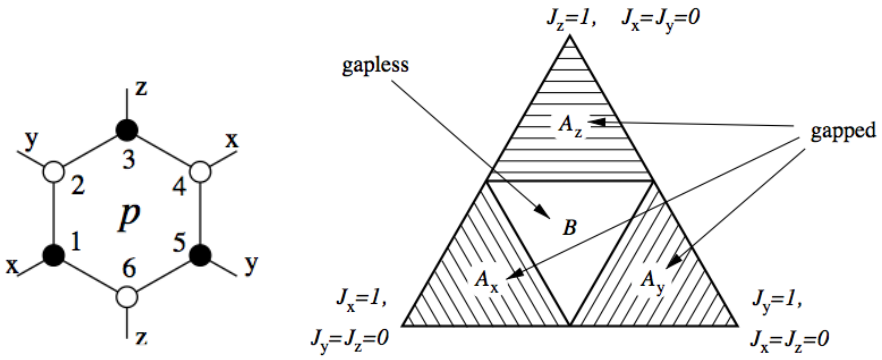

Fig. 5: *Left: Pictorial rendition of the local symmetry of Eq. (21) associated with every hexagon. Right: Phase diagram of the honeycomb Kitaev model. The triangle is the section of the positive octant* $(J_x, J_y, J_z) \geq 0$ *by the plane* $J_x+J_y+J_z = 1$. *The diagrams for the other octants are similar [45].*

the operators $\{O_{\hexagon_i}\}$, it suffices to allow the $N/2$ degrees of freedom η_{jk} on, for instance, all *vertical* bonds along $\boldsymbol{e}_3$ to attain a value of ± 1 and to pin η_{jk} on all other bonds (those along the $\boldsymbol{e}_1$ or $\boldsymbol{e}_2$ axis) to be 1. With this particular choice of the local gauge fields η, $\hat{O}_{\hexagon_i}$ in Eq. (23) reduces to the product of η_{jk} on the two vertical links that belong to each hexagon i.

The dimensionality of the original Hilbert space of N pseudo-spins is 2^N. Thus in each of the $2^{N/2}$ sectors of η_{jk}, there is a remaining Hilbert space of size $2^{N/2}$ on which the Majorana fermions are defined. One representation for the N Majorana fermions is in terms of $N/2$ spinless Dirac fermions. This may be explicitly done here by setting

$$c_j = d_{jk}+d_{jk}^\dagger \quad \text{and} \quad c_k = -i\big(d_{jk}-d_{jk}^\dagger\big), \tag{24}$$

with d_{jk} a spinless Dirac Fermi operator on the vertical link $\langle jk\rangle$ (that is, $k = j+\boldsymbol{e}_3$) [35]. The centers of the vertical links of the honeycomb lattice form a square lattice. It is therefore convenient to place the Fermi operators d_{jk} and $d_{jk}^\dagger$) at the centers of the vertical links $\langle jk\rangle$) and henceforth denote these by r, leaving us with the operators $d_r^\dagger$, d_r and the Ising degrees of freedom η_r. Denoting the unit vectors of the resulting square lattice by $\boldsymbol{e}_x$ and $\boldsymbol{e}_y$, the Kitaev Hamiltonian reduces to

$$H_{\hexagon}^K = J_x\sum_r \big(d_r^\dagger+d_r\big)\big(d_{r+\boldsymbol{e}_x}^\dagger-d_{r+\hat{e}_x}\big)+J_y\sum_r \big(d_r^\dagger+d_r\big)\big(d_{r+\hat{e}_y}^\dagger-d_{r+\hat{e}_y}\big)+J_z\sum_r \eta_r\big(2d_r^\dagger d_r-1\big). \tag{25}$$

The last term constitutes an analogue of a "minimal coupling" term between gauge (i.e., the fields η_r on vertical links emanating from sites r) and matter (fermionic) degrees of freedom that is familiar from electromagnetism – in this specific case, an analogue of a coupling between the charge (or matter) density and an electrostatic-type potential.

An advantage of the fermionization procedure employed above is that it does not require the use of elaborate non-local JW transformations. That the representation in terms of spinless fermions is $2^{N/2}$ dimensional can be checked by realizing that there are $N/2$ vertical links $\langle jk\rangle$ and the dimensionality of each spinless Fermion operator is two: the bond $\langle jk\rangle$ can be either occupied or un-occupied by a fermion. Putting all of the pieces together, one sees that the problem of solving $H_{\hexagon}^K$ has now been reduced to a problem involving solely fermions and Ising gauge degrees of

freedom η_r, which at each site r can only attain the value ± 1. All excitations that appear in this system can be expressed in terms of the original spin variables $\boldsymbol{\tau}_j$ or, equivalently, in terms of fermions and Ising gauge fields. The *fusion rules* that will appear both in this system and its non-Abelian extension that we will review in Sec. 3.4.2 must relate to *fermionic* and *Ising gauge* type basic degrees of freedom.

3.2.3 Ground state of fermionized model

Within the ground state sector, for all hexagons all $\hat{O}_{\hexagon_i} = 1$, or equivalently on the square lattice $\eta_r = 1$ for all sites r. That the ground state must be vortex free is ensured by a corollary of a theorem due to Lieb [67] and has also been established numerically [45]. In momentum space, the fermionized Hamiltonian of Eq. (25) assumes the form

$$H^K_{\hexagon} = \sum_{\boldsymbol{q}} \varepsilon_q \, d^\dagger_{\boldsymbol{q}} d_{\boldsymbol{q}} + i \frac{\Delta_{\boldsymbol{q}}}{2} \big(d^\dagger_{\boldsymbol{q}} d^\dagger_{-\boldsymbol{q}} + d_{\boldsymbol{q}} d_{-\boldsymbol{q}} \big), \tag{26}$$

where $\boldsymbol{q} = (q_x, q_y)$ and

$$\varepsilon_{\boldsymbol{q}} = 2J_z - 2J_x \cos q_x - 2J_y \cos q_y, \quad \Delta_{\boldsymbol{q}} = 2J_x \sin q_x + 2J_y \sin q_y. \tag{27}$$

Interestingly, this Hamiltonian has the form of a *p-wave BCS type Hamiltonian on the square lattice* [35], which becomes explicit when the Hamiltonian is cast in the form of a Bogoliubov-de Gennes (BdG) Hamiltonian

$$H^K_{\hexagon} = \begin{pmatrix} d^\dagger_{\boldsymbol{q}} & d_{-\boldsymbol{q}} \end{pmatrix} H^K_{BdG}(\boldsymbol{q}) \begin{pmatrix} d_{\boldsymbol{q}} \\ d^\dagger_{-\boldsymbol{q}} \end{pmatrix}, \tag{28}$$

where $H^K_{BdG}(\boldsymbol{q})$ is a 2×2 matrix. It can be cast in the slightly more general form

$$H_{BdG}(\boldsymbol{q}) = h_{\boldsymbol{q}} \sigma_x + \Delta_{\boldsymbol{q}} \sigma_y + \varepsilon_{\boldsymbol{q}} \sigma_z = \boldsymbol{d}(\boldsymbol{q}) \cdot \boldsymbol{\sigma}, \tag{29}$$

where $\boldsymbol{\sigma} = (\sigma_x, \sigma_y, \sigma_z)$ with Pauli matrices $\sigma_{x,y,z}$ and the last line defines the three-component vector $\boldsymbol{d}(\boldsymbol{q})$. Here an extra coupling $h_{\boldsymbol{q}}$ has been introduced for future reference. This coupling is not present within the pure honeycomb Kitaev model. Thus, $H^K_{BdG} = \lim_{h_{\boldsymbol{q}} \to 0} H_{BdG}(\boldsymbol{q})$.
In the Hamiltonian H_{BdG}, the vector $\boldsymbol{d}(\boldsymbol{q})$ acts as a "Zeeman field" applied to the "spin" $\boldsymbol{\sigma}$ of a two-level system. All of its eigenvalues come in pairs, at energies

$$E_{\boldsymbol{q}} = \pm d(\boldsymbol{q}) = \pm |\boldsymbol{d}(\boldsymbol{q})| = \pm \sqrt{\boldsymbol{d}(\boldsymbol{q}) \cdot \boldsymbol{d}(\boldsymbol{q})}. \tag{30}$$

Diagonalizing the Hamiltonian by a Bogoliubov transformation,

$$\gamma_{\boldsymbol{q}} = u_{\boldsymbol{q}} d_{\boldsymbol{q}} + v_{\boldsymbol{q}} d^\dagger_{-\boldsymbol{q}}, \tag{31}$$

with $|u_{\boldsymbol{q}}|^2 + |v_{\boldsymbol{q}}|^2 = 1$ and $|u_{\boldsymbol{q}}|^2 = \frac{1}{2}\sqrt{1 + \varepsilon_{\boldsymbol{q}}/E^2_{\boldsymbol{q}}}$, yields the energy spectrum

$$E_q = \pm \sqrt{\varepsilon_q^2 + |\tilde{\Delta}_q|^2}. \tag{32}$$

Note that no effective chemical potential appears here (i.e., $\mu = 0$). Thus, within the ground state, all fermionic states of negative energy ($E_q < 0$) are occupied while all states of positive energies are empty. The general ground state wavefunction corresponding to Eq. (32) is given by

$$|g\rangle = \prod_{\boldsymbol{q}} \left(u_{\boldsymbol{q}} + v_{\boldsymbol{q}} d^{\dagger}_{\boldsymbol{q}} d^{\dagger}_{-\boldsymbol{q}}\right)|0\rangle. \tag{33}$$

As mandated by particle-hole symmetry, non-zero eigenvalues of the BdG Hamiltonian of Eqs. (28) and (29) appear in *pairs*, at energies $\pm\varepsilon$ with $\gamma^{\dagger}_{-\varepsilon} = \gamma_{\varepsilon}$. Thus, generally, a fermion excitation eigenstate corresponds to two solutions of the BdG equations. At the energy $\varepsilon = 0$, the system is invariant under particle-hole symmetry, and a Majorana fermion appears (here $\gamma^{\dagger}_0 = \gamma_0$).

Whenever both ε_q and $\tilde{\Delta}_q$ vanish then a *Dirac node* may appear (i.e., the energy E_q will disperse linearly about its vanishing value at that point). Conversely, if for given J_x, J_y and J_z values there are no simultaneous solutions to the two conditions $\varepsilon_q = \tilde{\Delta}_q = 0$ then the spectrum will be gapped. In the vicinity of band extrema, the dispersions of Eq. (33) is parabolic when a gap appears between the two bands in the problem (i.e., $\min\{|E_q|\} > 0$) and, as just noted, is linear near the zeros of E_q when the system is gapless. Elementary calculations illustrate that when the moduli of the couplings $|J_x|, |J_y|$ and $|J_z|$ are such that they satisfy the triangle inequalities then the spectrum of Eq. (32) will be gapless. When the couplings violate the triangle inequalities, a gap emerges. The ground state of Eq. (33) corresponds to a BCS condensate. In [35], real space ground state wave-functions $|\Psi_0\rangle$ were explicitly constructed in the original spin representation in closed forms that do not require any implicit projections.

3.2.4 Gapless and gapped phases

To provide a better understanding of the spectrum, we focus on a particular set of couplings. At the symmetric system ($J_x = J_y = J_z$), the dispersion of Eq. (33) is, within the first Brillouin zone, zero at $\boldsymbol{q}^{(+)} \equiv \boldsymbol{K}_1/3 + 2\boldsymbol{K}_2/3, \boldsymbol{q}^{(-)} = 2\boldsymbol{K}_1/3 + \boldsymbol{K}_2/3$ where $\boldsymbol{K}_{1,2}$ denote the reciprocal lattice vectors along 1 and 2 directions [45] (and the equality holds modulo the addition of any reciprocal vectors). As the anisotropy of the coupling constants is increased (e.g., setting $|J_z|$ fixed and decreasing $|J_{x,y}|$), the two points $\boldsymbol{q}^{(\pm)}$ veer towards one another until they merge at the boundary between the gapped and gapless phases [45]. Beyond this point, as the $|J_{x,y}|$ are further decreased, and the system is in its gapped phase there are no real vectors $\boldsymbol{q}$ for which E_q is zero.

Similarly to the calculations above, the spectrum may be computed in other sectors of the Ising vortices. By looking at the algebra of the bonds appearing in the Hamiltonian, it is immediately clear that the spectrum is invariant under a change of sign of any of the exchange constants $J_\alpha \to -J_\alpha$. This, along with an overall global scale invariance of the gapless/gapped parameter regions under a uniform scaling of all coupling parameters $J_{x,y,z} \to cJ_{x,y,z}$ with c a constant enables us to delineate the boundaries of the gapless and gapped regions of the model. Such a phase diagram of the system is provided in Fig. 5 [45]. The existence of transitions between these phases are "topological" and as such cannot be discerned by any standard local measurements.

The inability of local measurements to discern between different phases underlies systems with topological order [16, 28, 34]. When expressed in terms of the basic spin degrees of freedom, anyons involve extended non-local lines. Amongst other probes, an interesting signature of the topological transitions between the Abelian phases in Kitaev's honeycomb model is afforded by quantum information theory measures, in particular the mutual information [68].
The condition for a gapless phase is tantamount to the triangle inequality via Eq. (27). This is so since (as alluded to in Section 3.2.3) the gapless phase implies $\varepsilon_q = \Delta_q = 0$ which in turn implies from Eq. (27) (via the law of cosines) that one can view q_x and q_y as angles in the triangle formed by the sides $\{J_x, J_y, J_z\}$ [35]. The relation between Kitaev's honeycomb model and the p-wave type pairing in Eqs. (25), (26) and (27) was further elucidated in several insightful works, [69, 70].

3.3 Braiding statistics

The Majorana fermion representation of Eq. (20) highlights another important property of this system – the braiding statistics formed by displacing one string of bonds around a closed loop. The product of bonds along any contour (open or closed) commutes with all other string products of the same form, including the symmetries O_h of Eqs. (21,23). That is, for any closed contour C drawn on the lattice, the operators

$$O_C = \prod_{ij \in C} b_{ij} \tag{34}$$

commute amongst themselves. For finite sized contours C, one has a sort of Stokes' theorem. That is, the symmetries of Eq. (34) can be written as [35]

$$O_C = \prod_{h \in C} O_h, \tag{35}$$

with the product taken over all hexagons h that are enclosed by the loop C. The right-hand side of Eq. (35) corresponds to the total anyonic charge enclosed by C. If an odd number of anyons (hexagons h for which $O_h = -1$) is circumscribed by C then $O_C = -1$. *This minus sign is the origin of the anyonic nature* of the braiding operations in Kitaev's model, e.g., [35, 71], in its gapped phase (known as the "A phase"). In the gapless phase of couplings of Kitaev's model ("B phase") the statistics of the vortices is ill defined. However, as will be elaborated on later, augmenting an additional external magnetic field term leads to the opening of a gap in the B phase. Within this gapped regime, the vortices exhibit well defined non-Abelian statistics.
An immediate corollary of the local ($d = 0$) symmetries O_h of Eqs. (21) and (23), is that, by Elitzur's theorem, only correlation functions that are invariant under all of these symmetries may attain a non-zero expectation value at finite temperatures [35]. Thus, all non-zero *correlation functions are composed of products of bonds (along closed or open contours) as in Eqs. (34) and (36).* Similar considerations also apply at zero-temperature. These considerations generally lead to string and "brane" type correlation functions. While the above considerations revolve around symmetries of the spins alone, an earlier work illustrated, by the use of Majorana fermions, that

all two-point correlation functions apart from those that form bonds vanish within the ground state and further related interesting consequences [72].
In the gapped phase, these string correlation functions are exponentially damped in spatial distance between the endpoints of the string (with a similar behavior concerning dynamic correlations). In the gapless phase, the string correlation functions decay algebraically in the distance. The striking difference between the slow algebraic vis-à-vis the rapid exponential decay of correlations is not limited only to the non-local string (or brane) correlation functions [35].

3.3.1 Fermion excitation and translation

The fermionization procedure discussed above enables the construction of anyons out of string operators [35]. A feature directly related to the symmetries of Eqs. (34) and (35) is that it is possible to create "fermionic" excitations alone sans anyons. One way to see this is by invoking symmetry and bond algebra arguments once again. Towards this end, one may consider the string product of bonds of the form of Eq. (34) yet now for *an open contour* Γ (as opposed to the closed contour C). That is, we may define the operator

$$O_\Gamma = \prod_{ij\in\Gamma} b_{ij} \tag{36}$$

along an open contour Γ. For the purposes of what follows, let us label the end points of Γ by U and V. Unlike O_c of Eq. (34), the operator of Eq. (36) is not a symmetry. That is, the operator O_Γ serves as a trivial symmetry for all bonds b_{kl} for which (1) $k, l \neq U$ or V and/or (2) lie along $\Gamma : k, l \in \Gamma$. For all such bonds, $[b_{kl}, O_\Gamma] = 0$. The above includes all bonds b_{kl} that have any number of sites along Γ (i.e., 0,1, or 2) such that the bonds do not touch Γ only at one point with that point being one of the endpoints U or V. However, if $k = U$ or V and $l \notin \Gamma$ or vice versa (i.e., $l = U$ or V and $k \notin \Gamma$) then b_{kl} will anti-commute with O_Γ:

$$\left\{O_\Gamma,\, b_{kl}\right\} = 0. \tag{37}$$

There are four such bonds b_{kl}. All other bonds commute with the operator of Eq. (36), $[O_\Gamma, b_{mn}] = 0$. As the exact solution that was outlined earlier [Eqs. (27), (33)] shows, the ground state sector of Kitaev's model is not highly degenerate. As O_Γ flips the energetic contributions of the four bonds b_{kU} and b_{Vl} that touch the endpoints U and V, all of this suggests that the application of general O_Γ (there is an exponentially large number of contours Γ) on a ground state cannot give back a ground state but rather must excite the system. The bonds at the end points of the contour Γ have been modified (by a change of sign) as a result of the anticommutation relation of Eq. (37) and together the four disrupted bonds at the two endpoints U and V that do not lie along Γ sum to yield a higher energy state. Thus, it is natural to associate defects created by the string operator of Eq. (36) at the endpoints U and V of the contour Γ. As seen from Eqs. (20) and (36), the string operator O_Γ involves only the Majorana fermions and not the anyons of Eqs. (21), (23) and their composites Eq. (35). Indeed, it is possible to verify that as each of the bonds of the lattice, b_{ij} of Eqs. (19) and (20) commutes with all anyonic charges

O_h of Eqs. (21) and (23), the operator of Eq. (36) does not create (nor, in general, remove or displace) any anyons: $[O_\Gamma,\, O_h] = 1$. For a closed loop however, the closed string operator of Eqs. (34) and (35) is a symmetry. The existence of general $d = 1$ symmetry operators that are products of defect creation operators along loops [28] has similar incarnations elsewhere (e.g., in quantum Hall systems with the creation of quasi-particle/quasi-particle pairs). By creating defects and moving these defects along entire closed cycles, the defects annihilate and the system returns to its low energy (ground state) sector. Putting all of the pieces together, one sees that it is possible to have fermionic excitations (generated by Eq. (36)) alone. It is possible to express all of these results in terms of the fermions directly similar to [35].
When a fermion is transported around a closed loop that encircles a single Ising vortex (for which $O_h = -1$), we see that Eqs. (34) and (35) reduce to an overall phase factor of -1. Thus, in such an instance the quantum state is multiplied by this overall phase factor [45].

3.3.2 Vortex pair creation and translation

It is common to think about excitations formed by the application of single spin operators (i.e., by a rotation of a single spin) or by a product of two on the ground state. As pointed out by [73], there are subtleties associated with a simple interpretation of the action of these operations within the low energy sector. In what follows, we will focus on such an excitation via general symmetry and bond algebraic considerations. Towards this end, we consider a single vertical link (ij). We define, similarly to [45, 74, 75], the three operators $X = \sigma_i^x \sigma_j^x$, $Y = \sigma_i^x \sigma_j^y$, and $Z = \sigma_j^z$. These operators are different from those of Eq. (36) (including the case of a single two site bond). Each of these three operators anti-commutes with two bond operators. For instance, Z anticommutes with the two bonds (other than b_{ij}) that have j as one of their endpoints. Similarly, the operators X and Y each anti-commute with exactly two bonds. When acting on the ground state, the flipping operations incurred by any of the operators X, Y or Z may increase the system energy. It is furthermore readily verified that Y and Z may each flip the anyonic charges O_h of two hexagonal plaquettes while X flips the anyonic charges of all four hexagonal plaquettes that contain either the site i or j (or both). The flipping of any of the bonds generated by each of these three operators can be accounted for by inverting the sign of the η field along the corresponding link following Eq. (20). The three operators satisfy the $S = 1/2$ spin algebra:

$$\{X, Y\}{=}\{X, Z\}{=}\{Y, Z\} = 0, \;\; X^2{=}Y^2{=}Z^2 = 1, \text{ and } \; XY{=}iZ, \; YZ{=}iX, \; ZX{=}iY. \quad (38)$$

It is natural to associate "particles" with states $X|\psi\rangle, Y|\psi\rangle, Z|\psi\rangle$ created by the application of the operators X, Y or Z on the ground state wavefunction. The identities of Eq. (38) generally suggests that a fusion of two particles into a third might be possible. This is indeed the case as has been worked out in some detail in various approaches and limits (especially that of $J_z \gg J_{x,y}$ lying within the A phases of the system, see Fig. 5 [45, 75]. In that limit, the energy of the excitation $X|\psi\rangle$ is nearly equal to the sum of energies corresponding to $Y|\psi\rangle$ and $Z|\psi\rangle$.
As the anyonic charges of Eq. (21) are symmetries, anyonic excitations are massive. That is, an anyonic excitation is stationary as it is an eigenstate of the Hamiltonian. As discussed in [73],

it is possible to create anyons without fermions by the combined use of one and three spin operations on the ground state. We now extend the discussion of the single bond operators above and present the general vortex translation (or anyon) operator. An approach related to ours, along with a detailed analysis of energies, is given in [71]. An insightful analysis is also provided in [73]. In order to analyze the Ising vortex translation operators, we introduce an operator that is identical to that of Eq. (36) apart from all important end point corrections that allow it to be expressed as O_Γ multiplied by two operators corresponding to the two endpoints. Specifically, we consider an open contour Γ. For each non endpoint vertex $i \in \Gamma$, there is only a single neighbor l that is not on Γ. For the two end points of Γ ($i_1 = U$ and $i_2 = V$), there are two neighbors l that do not lie on Γ. One may choose any of these neighbors for the two endpoints in what follows. (We will mark the chosen neighbors for the endpoints by l_1 and l_2 respectively.) We denote the direction of a ray parallel to the nearest neighbor link $\langle il \rangle$ by γ (that may be either x, y, or z). We then construct the open contour operator

$$\mathcal{T}_\Gamma = \prod_{i \in \Gamma} \sigma_i^\gamma. \tag{39}$$

Eq. (39) is of nearly identical form to (36) for all non-boundary points i. However, in Eq. (36), the component of the boundary spin operators that appear in the string operator are set equal to the two directions $\gamma_{1,2} = \langle i_{1,2} j_{1,2} \rangle$ with $j_{1,2}$ being the nearest neighbors of $i_{1,2}$ that *lie on* Γ (i.e., "going backwards" away from the endpoints $i_{1,2}$). By contrast, in Eq. (39), the components of the spins at the two endpoints that appear in the string product are set by the two directions $\gamma = \langle i_{1,2} l_{1,2} \rangle$ (with $l_{1,2}$ not on Γ).

For the two hexagonal plaquettes $h^* = h_{1,2}$ that have a single vertex at one of the endpoints of i_1 or i_2 of Γ and that furthermore include one of the vertices l_1 or l_2, we have that

$$\mathcal{T}_\Gamma O_{h*} \mathcal{T} = -O_{h^*}. \tag{40}$$

In Eq. (40), O_{h*} denotes the vortex charge of a plaquette $h*$ that lies at an endpoint of Γ. Similar to the operator of Eq. (36), for all other plaquettes $h \neq h^*$, we have that $\mathcal{T}_\Gamma O_h \mathcal{T}_\Gamma = O_h$ (with no change in the vortex charge).

It is readily verified that the operator $\mathcal{T}_\Gamma$, albeit flipping the sign of two bonds attached to the endpoints of Γ, does *not alter* the bond algebra of all bonds (all non-neighboring bonds commute, neighboring bonds anticommute, and the square of any bond is 1). The sole change triggered by the application of $\mathcal{T}_\Gamma$ is that two bond pre-factors η are multiplied by a factor of -1, and correspondingly two vortex charges are flipped. Thus, the effect of $\mathcal{T}_\Gamma$ is to flip the sign of the two vortices at its endpoints.

If the system has a single vortex $O_{h_1} = -1$ at plaquette h_1 that has only one (endpoint) on Γ and furthermore contains one of the two points $l_{1.2}$, then the application of $\mathcal{T}_\Gamma$ with the contour Γ having a single point in the plaquette h_1 (the latter plaquette also containing the point l_1) as one of its endpoints will move the vortex to another plaquette h_2 that lies at the other end of the contour Γ (and contains the point l_2). That is, $\mathcal{T}_\Gamma$ is a *vortex translation operator*. If Γ forms a complete closed contour C along a toric cycle (when h_1 and h_2 are identified as the same point

on the torus) then, similarly to O_Γ of Eq. (36), $\mathcal{T}_\Gamma$ veers towards the $d = 1$ dimensional symmetry of Eq. (34). In the above, we established that the sole effect of $\mathcal{T}_\Gamma$ is to displace a vortex without influencing the system energy from any of the bonds that do not touch the endpoints of the contour Γ.

3.4 Broken time reversal symmetry – the non-Abelian phase

Kitaev's model for a wide range of couplings corresponds, as discussed earlier to a gapless phase, the so-called "B" phase. It is only in the "corners" of the phase diagram of Fig. 5 (the so-called "A" phase where the $\{J_x, J_y, Jz\}$ differ substantially from one another and cannot form the sides of a triangle) that a gap opens up. In the A phase, gapped Abelian anyons are present. Our focus in this section will be on the B phase where gapless excitations of Eq. (33) were found. By a modification of Kitaev's honeycomb model, gapped non-Abelian excitations can arise. There are various ways in which such excitations can arise. For instance, these may be triggered by the geometry of the lattice (via, e.g., a decoration of the lattice wherein each vertex of the hexagonal lattice is replaced by a triangle [76]). In what follows, we consider the original investigation of [45] in which a gapped phase with non-Abelian excitations originates from the application of an external magnetic field to a point (J_x, J_y, J_z) in the space of coupling constants for which the system would have been gapless if no field were applied.

In the context of the broad link to topological insulator physics and, in particular, to the symmetry classification of topological insulators [77–79, 5], in the absence of any additional perturbations, the free fermion Kitaev honeycomb model lies in the "BDI" symmetry class. In the presence of an external field time reversal breaking field, however, the symmetry becomes that of the "D" class raising the specter of a non-trivial insulator as indeed occurs in the nontrivial B phase of the extended Kitaev model. As we now review, such a time reversal symmetry breaking field gives rise to an effective *next nearest neighbor coupling* between Majorana fermions. This additional hopping leads to a gapped spectrum with non-Abelian chiral modes. When a magnetic field $\boldsymbol{h}$ is applied along the $[111]$ direction, i..e., when Eq. (17) is augmented by a Zeeman coupling

$$H' = H - \sum_i \boldsymbol{h} \cdot \boldsymbol{\tau}_i, \tag{41}$$

a gap opens up in the core region (B phase) of the phase diagram of Fig. 5. The (time reversal broken) phase that arises from the application of this field is very interesting.

In particular, non-Abelian anyons appear in the former gapless phase (which includes the symmetric point $J_x = J_y = J_z$). The Hamiltonian of Eq. (41) is not exactly solvable. It can, however, be treated perturbatively and (ignoring unimportant corrections) reduced to an exactly solvable system [45]. That is, the magnetic field term in Eq. (41) gives rise (with $\kappa \sim h_x h_y h_z / J^2$ in the symmetric point $J_x = J_y = J_z = J$) to a (time reversal symmetry breaking) term of the form of Eq. (18) which we write here anew,

$$H_h = -\kappa \sum_{ijk} \sigma_i^x \sigma_j^y \sigma_k^z, \tag{42}$$

for all triplets of sites (i, j, k) formed by the union of the two bonds, (ij) and (jk), that impinge on site j. The *product of the three spin operators* of Eq. (42) can be expressed as a *product of two neighboring bonds* of Eqs. (19) and (22) by use of the relation $c_j^2 = 1/2$. For instance, for (oriented) links (ij) and (jk) along the x and z directions respectively (with $i_z < j_z$ and $j_z < k_z$), the product of the bonds of Eq. (22) reads $b_{ij}b_{jk} = -2\eta_{ij}\eta_{jk}c_ic_k$. Eq. (42) is seen to reduce to a *Majorana fermion bi-linear linking (all) next nearest neighbor sites*. The Majorana fermion bi-linear (c_ic_k) resulting from the product of two bonds has a real prefactor $(-2\eta_{ij}\eta_{jk})$ as opposed to the imaginary prefactors that are associated with single nearest neighbor bonds in Eq. (22). This relative phase factor of i reflects the time reversal symmetry breaking of the perturbation. Time reversal symmetry breaking also allows for the existence of chiral modes wherein fermionic modes may preferentially propagate in one (clockwise or anti-clockwise) direction. For any pair of next nearest neighbor sites (ik) on the honeycomb lattice, there is a unique three site path (and two bond product) that leads to the bi-linear form c_ic_k. The quadratic character of these three-spin perturbations of Eq. (42) in the Majorana fermions (and similarly also in the fermions following, e.g., Eq. (24)) ensures that even when the system is augmented by these perturbations, the final Hamiltonian

$$H_{K_h;h} \equiv H_{K_h} + H_h \tag{43}$$

formed by the sum of Eqs. (17) and (42) is *still exactly solvable*.

3.4.1 Solution of extended model with broken time reversal symmetry

The solution to the problem is of a similar character to the one that earlier led to Eqs. (27) and (33). As each spin product of the type $\sigma_i^x\sigma_j^y\sigma_k^z$ is given by a product of two bonds (each of which commutes with all of the symmetries of Eq. (21), it follows that the perturbation of Eq. (42) commutes with the operators O_h. As before, in any given sector one can employ the representation of Eqs. (19) with η related to the flux via the condition of Eq. (23). All of the earlier steps taken in Eqs. (27) and (26) can thus be exactly reproduced. However, unlike the nearest neighbor Hamiltonian that we studied earlier in the absence of an applied external field h (or an effective), the next-nearest neighbor Fermi interactions lead to new non-trivial results. In particular, the perturbation set non-zero $\boldsymbol{h}$ allows the earlier gapless phase in the absence of a field to become gapped and thus to support anyons which within this phase are non-Abelian [45]. The spectrum of $H_{K_h;h}$, in the vortex free sector ($O_h = 1$ for all h) is then seen to be given by Eq. (32) where the real p-wave type gap Δ_q [35] of Eq. (27) is now replaced by the complex

$$\tilde{\Delta}_q = \Delta_q + 4i\kappa\big(\sin q_1 - \sin q_2 + \sin(q_2 - q_1)\big). \tag{44}$$

As can be seen by some simple analysis, the former gapless points $\boldsymbol{q}^{(\pm)}$ of Eq. (33) now acquire a gap when $\kappa \neq 0$. The p-wave type gap function $\tilde{\Delta}$ now becomes complex [35]. This suggests that the physics will essentially be the same as that for $(p+ip)'$ superconductors [51] which is indeed the case. It is noteworthy that even when the Hamiltonian is time reversal invariant the ground states may spontaneously break time reversal. Indeed, by Kramers' theorem, this must

occur whenever the system is defined on a hexagonal lattice with an odd number of spins [35]. In the B phase of Kitaev's model wherein the gap was borne by the perturbation, the associated Chern number $\nu = \pm 1$ and the aforementioned non-trivial statistics [45] with non-Abelian topological anyons. We elaborate on these anyons and their features next.

3.4.2 Non-Abelian anyons in Kitaev's model and their properties

To conform with standard practice, we use σ to denote a vortex (defined, similarly to the Abelian phase, by having the plaquette product O_h of Eqs. (21) and (23) be -1, $O_h = -1$), ε to mark a fermionic mode, and I to denote the vacuum (having no anyons). The fusion rules are then of the form

$$\varepsilon \times \varepsilon = I, \quad \sigma \times \varepsilon = \sigma, \text{ and } \sigma \times \sigma = I + \varepsilon, \tag{45}$$

augmented by the trivial statement that the fusion of any particle with the identity operator leads back to that particle. As in the case of the Abelian anyons each particle is its own anti-particle. The non-trivial character of the non-Abelian anyons rears its head in the last line of Eq. (45). Two vortices (σ) may fuse in two different channels to either annihilate (I) each other or to form a fermion (ε). The vortex operators of Eq. (21) have, as always, Ising eigenvalues $O_h = \pm 1$. Anyons that satisfy the relations of Eq. (45) are called "Ising anyons". Unlike the case of Abelian anyons, *fusing two anyons may lead to non-unique outcomes*. In particular, if particles a and b are fused when $a = b = \sigma$ then this may yield an ε particle or the vacuum (I). In the limit of spatially infinitely distant vortices, the fermionic spectrum as adduced from the square lattice Hamiltonian with η_r on the vertical links of original the honeycomb lattice set by the vortices O_h of Eq. (23), exhibits a multitude of fermionic *zero modes* [80]. Thus the hybrid of two well separated vortices (σ) may lead to a state in which the vortices annihilate to form the vacuum (I) or a "zero energy" fermionic state (ε). This degeneracy is lifted once the vortices become close to one another wherein the fermionic modes ε attain a finite energy cost (or "mass"). Repeated applications of the last of Eqs. (45) rationalizes the $2^{n_\sigma/2-1}$-fold degeneracy that is present in a system of n_σ (with this number being an even integer) well separated vortices [81]. In formal terms, the quantum dimension of the vortices σ is $d_\sigma = \sqrt{2}$; the system degeneracy for n_σ vortices scales as $d_\sigma^{n_\sigma}$. Due to the unique outcome of all of the other fusion rules in Eq. (45), the quantum dimensions of ε and I are $d_\varepsilon = d_I = 1$.

References

[1] K. Kugel and D. Khomskii, Sov. Phys. Usp. **25**, 231 (1982)

[2] G. Jackeli and G. Khaliullin, Phys. Rev. Lett. **102**, 017205 (2009)

[3] J. Chaloupka, G. Jackeli, and G. Khaliullin, Phys. Rev. Lett. **105**, 027204 (2010)

[4] Z. Nussinov and J. van den Brink, Rev. Mod. Phys. **87**, 1 (2015)

[5] S. Trebst, Phys. Rep. **950**, 1 (2017)

[6] Z. Nussinov and E. Fradkin, Phys. Rev. B **71**, 195120 (2005)

[7] Z. Nussinov and G. Ortiz, Europhysics Lett. **84**, 36005 (2008)

[8] V.W. Scarola, K.B. Whaley, and M. Troyer, Phys. Rev. B **79**, 085113 (2009)

[9] C. Xu and J.E. Moore, Nucl. Phys. B **716**, 487 (2005)

[10] C. Xu and J.E. Moore, Phys. Rev. Lett. **93**, 047003 (2004)

[11] J.E. Moore and D.-H. Lee, Phys. Rev. B **69**, 104511 (2004)

[12] E. Cobanera, G. Ortiz, and Z. Nussinov, Phys. Rev. Lett. **104**, 020402 (2010)

[13] X.-G. Wen: *Quantum Field Theory of Many-Body Systems* (Oxford University Press, 2004)

[14] F. Wegner, J. Math. Phys. **12**, 2259 (1971)

[15] J.B. Kogut, Reviews of Modern Physics **51**, 659 (1979)

[16] A.Y. Kitaev, Ann. Phys. **303**, 2 (2003)

[17] E. Fradkin and S.H. Shenker, Phys. Rev. D **19**, 3682 (1979)

[18] Z. Nussinov, Phys. Rev. D **72**, 054509 (2005)

[19] V.J. Emery, E. Fradkin, S.A. Kivelson, and T.C. Lubensky, Phys. Rev. Lett. **85**, 2160 (2000)

[20] A. Vishwanath and D. Carpentier, Phys. Rev. Lett. **86**, 676 (2001)

[21] E. Fradkin and S.A. Kivelson, Phys. Rev. B **59**, 8065 (1999)

[22] A.H. MacDonald and M.P.A. Fisher, Phys. Rev. B **61**, 5724 (2000)

[23] A. Paramekanti, L. Balents, and M.P.A. Fisher, Phys. Rev. B **66**, 054626 (2002)

[24] J.W.F. Venderbos, M. Daghofer, J. van den Brink, and S. Kumar, Phys. Rev. Lett. **107**, 076405 (2011)

[25] D. Gaiotto, A. Kapustin, N. Seiberg and B. Willett, J. High Energy Phys. **2015**, 172 (2015)

[26] C.D. Batista and Z. Nussinov, Phys. Rev. B **72**, 045137 (2005)

[27] Z. Nussinov, G. Ortiz, and E. Cobanera, Ann. Phys. **327**, 2491 (2012)

[28] Z. Nussinov and G. Ortiz, Proc. Nat. Acad. Sci. U.S.A. **106**, 16944 (2009)

[29] C. Batista and S. Trugman, Phys. Rev. Lett. **93**, 217202 (2004)

[30] Z. Nussinov, C.D. Batista, B. Normand, and S.A. Trugman, Phys. Rev. B **75**, 094411 (2007)

[31] Z. Nussinov and G. Ortiz, Phys. Rev. B **107**, 045109 (2023)

[32] Z. Nussinov, C. Batista, and E. Fradkin, Int. J. Mod. Phys. B **20**, 5239 (2006)

[33] S. Elitzur, Phys. Rev. D **12**, 3978 (1975)

[34] Z. Nussinov and G. Ortiz, Ann. Phys. **324**, 977 (2009)

[35] H.-D. Chen and Z. Nussinov, J. Phys. A **41**, 075001 (2008)

[36] D. Perez-Garcia, M.M. Wolf, M. Sanz, F. Verstraete, and J.I. Cirac, Phys. Rev. Lett. **100**, 167202 (2008)

[37] J. Villain, Solid State Comm. **10**, 967 (1972)

[38] E. Shender, Sov. Phys. JETP **56**, 178 (1982)

[39] C. Henley, Phys. Rev. Lett. **62**, 2056 (1989)

[40] Z. Nussinov, M. Biskup, L. Chayes, and J. van den Brink, Europhys. Lett. **67**, 990 (2004)

[41] M. Biskup, L. Chayes, and Z. Nussinov, Commun. Math. Phys. **255**, 253 (2005)

[42] B. Doucot, M. Feigel'man, L. Ioffe, and A. Ioselevich, Phys. Rev. B **71**, 024505 (2005)

[43] J. Dorier, F. Becca, and F. Mila, Phys. Rev. B **72**, 024448 (2005)

[44] F. Lin and V.W. Scarola, Phys. Rev. Lett. **111**, 220401 (2013)

[45] A.Y. Kitaev, Ann. Phys. **321**, 2 (2006)

[46] Z. Nussinov and G. Ortiz, Phys. Rev. B **77**, 064302 (2008)

[47] S. Sachdev, arXiv:0901.410

[48] T. Senthil and M.P.A. Fisher, Phys. Rev. B **63**, 134521 (2001)

[49] J. Linder, Y. Tanaka, T. Yokoyama, A. Sudbo, and N. Nagaosa, Phys. Rev. Lett. **104**, 067001 (2010)

[50] N. Read and D. Green, Phys. Rev. B **61**, 10267 (2000)

[51] D.A. Ivanov, Phys. Rev. Lett. **86**, 268 (2001)

[52] J. Alicea, Phys. Rev. B **81**, 125318 (2010)

[53] J. Alicea, Y. Oreg, G. Refael, F. von Oppen, and M.P.A. Fisher, Nat. Phys. **7**, 412 (2011)

[54] J.D. Sau, R.M. Lutchyn, S. Tewari, and S. Das Sarma, Phys. Rev. Lett. **104**, 040502 (2010)

[55] H.-D. Chen, C. Fang, J. Hu, and H. Yao, Phys. Rev. B **75**, 144401 (2007)

[56] X.-Y. Feng, G.-M. Zhang, and T. Xiang, Phys. Rev. Lett. **98**, 087204 (2007)

[57] G. Kells, J.K. Slingerland, and J. Vala, Phys. Rev. B **80**, 125415 (2009)

[58] J. Vidal, K.P. Schmidt, and S. Dusuel, Phys. Rev. B **78**, 245121 (2008)

[59] F.J. Burnell and C. Nayak, Phys. Rev. B **84**, 125125 (2011)

[60] R. Schaffer, S. Bhattacharjee, and Y.-B. Kim, arXiv:1206.5814 (2012)

[61] Z. Nussinov and G. Ortiz, Phys. Rev. B **79**, 214440 (2009)

[62] E. Cobanera, G. Ortiz, and Z. Nussinov, Advances in Physics **60**, 679 (2011)

[63] W. Brzezicki and A.M. Oleś, European Physical Journal B **66**, 361 (2008)

[64] E. Eriksson and H. Johannesson, Phys. Rev. B **79**, 224424 (2009)

[65] J. Vidal, R. Thomale, K.P. Schmidt, and S. Dusuel, Phys. Rev. B **80**, 081104(R) (2009)

[66] V. Karimipour, Phys. Rev. B **79**, 214435 (2009)

[67] E.H. Lieb, Phys. Rev. Lett. **73**, 2158 (1994)

[68] J. Cui, C. Jun-Peng, and H. Fan, Physical Review A **82**, 022319 (2010)

[69] Y. Yu and Z. Wang, Europhysics Letters **84**, 57002 (2008)

[70] Y. Yu, Nuclear Physics B **799**, 345 (2008)

[71] G. Kells, A.T. Bolukbasi, V. Lahtinen, J.K. Slingerland, J.K. Pachos, and J. Valla, Phys. Rev. Lett. **101**, 240404 (2008)

[72] G. Baskaran, S. Mandal, and R. Shankar, Phys. Rev. Lett. **98**, 247201 (2007)

[73] S. Dusuel, K.P. Schmidt, and J. Vidal, Phys. Rev. Lett. **100**, 177204 (2008)

[74] J.K. Pachos, Int. J. Quantum Inf. **4**, 947 (2006)

[75] J.K. Pachos, Ann. Phys. **322**, 1254 (2007)

[76] H. Yao and S.A. Kivelson, Phys. Rev. Lett. **99**, 247203 (2007)

[77] P. Schnyder, A., S. Ryu, A. Furusaki, and A.W.W. Ludwig, Phys. Rev. B **78**, 195125 (2008)

[78] A. Kitaev, AIP Conference Proceedings **1134**, 22 (2009)

[79] S. Ryu, A.P. Schnyder, A. Furusaki, and A.W.W. Ludwig, New J. Phys. **12**, 065010 (2010)

[80] V. Lahtinen, G. Kells, A. Carollo, T. Stitt, J. Vala, and J.K. Pachos, Ann. Phys. **323**, 2286 (2008)

[81] C. Nayak and F. Wilczek, Nucl. Phys. B **479**, 529 (1996)